European Journal of Medicinal Chemistry 302 (2026) 118291

Contents lists available at ScienceDirect

European Journal of Medicinal Chemistry

journal homepage: www.elsevier.com/locate/ejmech

Research paper

Production, crystallographic studies, and functional profiling of γ-carbonic anhydrase from the probiotic *Limosilactobacillus reuteri*: *In vitro* and cell-based insights

Alessandro Bonardi [a,b], Simone Carradori [c,d,*], Niccolò Paoletti [a,b], Andrea Angeli [a], Marta Ferraroni [e], Damiano Iacovozzi [c], Marialucia Gallorini [c], Ilaria D'Agostino [f], Viviana De Luca [g], Paola Gratteri [b], Amelia Cataldi [c,d], Claudiu T. Supuran [a], Clemente Capasso [g]

[a] *NEUROFARBA Department, Section of Pharmaceutical and Nutraceutical Sciences, University of Florence, Polo Scientifico, Via U. Schiff 6, Sesto Fiorentino, Firenze, 50019, Italy*
[b] *NEUROFARBA Department, Section of Pharmaceutical and Nutraceutical Section, Laboratory of Molecular Modeling Cheminformatics & QSAR, University of Florence, Via U. Schiff 6, Sesto Fiorentino, Firenze, 50019, Italy*
[c] *Department of Pharmacy, "G. d'Annunzio" University of Chieti-Pescara, via dei Vestini 31, Chieti, 66100, Italy*
[d] *UdA-TechLab, "G. d'Annunzio", University of Chieti-Pescara, Chieti, 66100, Italy*
[e] *Department of Chemistry "Ugo Schiff", University of Florence, Via della Lastruccia 3-13, Sesto Fiorentino, 50019, Italy*
[f] *Department of Pharmacy, University of Pisa, via Bonanno Pisano 6, Pisa, 56126, Italy*
[g] *Department of Biology, Agriculture and Food Sciences, CNR, Institute of Biosciences and Bioresources, Napoli, 80131, Italy*

ARTICLE INFO

Keywords:
Activators
Carbonic anhydrase
Inhibitors
Kinetics profiling
Lactobacillus reuteri
Macrophages
Recombinant proteins

ABSTRACT

Limosilactobacillus reuteri (formerly *Lactobacillus reuteri*) is a probiotic bacterium involved in maintaining gut microbiota balance and modulating immune response. In this study, for the first time, we report the recombinant production and kinetic characterization of its γ-class carbonic anhydrase (CA, EC 4.2.1.1), referred to as LreCAγ. The enzyme catalyzes CO_2 hydration with an efficiency comparable to that of other bacterial γ-CAs, although lower than that of α-hCA II. X-ray crystallization studies shed light on the enzyme structure, and inhibition studies with anions, sulfonamides, and related compounds revealed that LreCAγ is less susceptible to inhibition compared to the γ-class CA from *Vibrio cholerae*, used for comparison. Otherwise, activation assays with selected amines and amino acids identified the two enantiomers of His (**25** and **26**) as the most potent LreCAγ activators. Stereochemistry had a minimal impact on activity, except for *L*-Phe (**27**), which was twice as potent as its *D*-enantiomer (**28**). To assess the biological effects of CA modulation, *E. coli* DH5α, which expresses several CAs, was used as a model organism. CA activators were tested alone and in combination with the pan-CA inhibitor acetazolamide (**AAZ**), revealing CA-dependent effects on bacterial growth. Additionally, selected CA activators were evaluated for their effects on human macrophages and intestinal epithelial cells, with *L*-Trp (**31**) attenuating LPS-induced activation and exhibiting good biocompatibility in normal intestinal cells. Taken together, these results underscore the feasibility of targeting LreCAγ activation as a strategy to enhance probiotic efficacy.

1. Introduction

The human microbiota comprises at least 100 trillion microbial cells, playing a fundamental role in host physiology, metabolism, immunity, and protection [1]. Emerging high-throughput sequencing technologies have expanded the understanding of gut-resident microorganisms, including bacteria, archaea, eukaryotes, and viruses [2]. Among them, probiotics are defined as live microorganisms that promote host health,

* Corresponding author. Department of Pharmacy, "G. d'Annunzio" University of Chieti-Pescara, via dei Vestini 31, 66100 Chiety, Italy.
E-mail addresses: alessandro.bonardi@unifi.it (A. Bonardi), simone.carradori@unich.it (S. Carradori), niccolo.paoletti@unich.it (N. Paoletti), andrea.angeli@unifi.it (A. Angeli), marta.ferraroni@unifi.it (M. Ferraroni), damiano.iacovozzi@phd.unich.it (D. Iacovozzi), marialucia.gallorini@unich.it (M. Gallorini), ilaria.dagostino@unipi.it (I. D'Agostino), vivianadeluca@cnr.it (V. De Luca), paola.gratteri@unifi.it (P. Gratteri), amelia.cataldi@unich.it (A. Cataldi), claudiu.supuran@unifi.it (C.T. Supuran), clemente.capasso@cnr.it (C. Capasso).

https://doi.org/10.1016/j.ejmech.2025.118291
Received 9 September 2025; Received in revised form 13 October 2025; Accepted 20 October 2025
Available online 25 October 2025

particularly by restoring microbiota balance after antibiotic therapy [3].

In recent years, probiotics have garnered interest due to their documented beneficial effects in a wide range of pathological conditions [4], demonstrating a therapeutic or preventive role in gastrointestinal disorders such as irritable bowel syndrome (IBS), antibiotic-associated diarrhea, and infectious enterocolitis [5]. Moreover, emerging research supports their involvement in modulating systemic conditions, including metabolic syndromes, allergic reactions, neurodevelopmental disorders, and even certain psychiatric conditions, via the gut-brain axis [6,7]. As a result, the use of probiotics has expanded far beyond conventional food supplements, with current formulations being integrated into functional foods and pharmaceutical agents [8–10].

However, given the complexity of the gut ecosystem and the variability in host response, there is a growing demand for innovative strategies to enhance the safety and stability, along with colonization efficiency and overall functional performance of probiotic strains [11–13]. Interestingly, these research trends seem to underscore the strategic value of probiotics as therapeutic allies, not only in gut health but also in the broader context of preventive medicine [14,15].

Our research group has longstanding expertise in the production, kinetic analysis, and biochemical characterization of carbonic anhydrases (CAs, EC 4.2.1.1) [16], focusing on their exploitation as pharmacological and druggable targets for a variety of biomedical applications [17–19], including cancer [20,21], infectious diseases [22–24], and neurological disorders [25–27]. CAs are a superfamily of metalloenzymes encoded by most living organisms, including humans, pathogenic and beneficial bacteria. They catalyze the reversible hydration of carbon dioxide (CO_2) to bicarbonate (HCO_3^-) and protons (H^+), a fundamental reaction that supports key biosynthetic and physiopathological pathways [28–30]. Among the eight known CA classes, the α, β, γ, and ι ones are expressed in bacteria [31]. In recent decades, growing evidence has highlighted the pivotal role of bacterial CAs in survival, virulence, adaptation to environmental changes, biofilm formation, and pH regulation [32]. In light of these roles, our group has developed several selective inhibitors designed to impair bacterial viability and virulence by targeting their CA activity [33–36]. In general, the emerging antibacterial strategy of targeting CAs in bacterial pathogens is highly attractive [37,38]. However, it undoubtedly requires a great effort in designing highly selective inhibitors to minimize off-target effects on probiotic strains, in order to avoid the impairment of their physiological functions [39]. This consideration is particularly relevant in the context of gastrointestinal infections, where pathogenic and probiotic bacteria coexist in the same anatomical compartment. In such cases, maintaining the activity of probiotic strains may be essential for preserving gut balance and enhancing recovery. A notable example is *Vibrio cholerae*, a human gastrointestinal pathogen that causes cholera. This bacterium encodes three CA isoforms, α-, β-, and γ-class enzymes, referred to as VchCAs. These enzymes contribute to the production of bicarbonate ions, which are crucial for the optimal expression and activity of cholera toxin (CTX), a key virulence factor involved in disease progression [24,40–43]. Therefore, targeting VchCAs with selective inhibitors could reduce pathogenicity by interfering with this bicarbonate-dependent mechanism, while ideally sparing the CAs of beneficial gut microbiota [44].

However, although several probiotic CAs have been reported in the UniProtKB database (https://www.uniprot.org) [45], there is no comprehensive understanding of their specific roles and contributions to the survival, metabolism, and performance of such probiotic microorganisms. In this context, we began to explore whether the activation of CAs in probiotic strains, an emerging field of study [46–53], could represent a promising strategy to enhance their enzymatic activity and, potentially, improve the overall probiotic performance, in the search for preventive or antibiotic-adjuvant therapies. This hypothesis remains largely unexplored due to the limited scientific literature currently available in this field. To initiate investigation in this direction, we selected *Limosilactobacillus reuteri* (formerly *Lactobacillus reuteri*), a Gram-positive, facultative anaerobic bacterial strain belonging to the human microbiome, with significant levels present within the small intestine and feces of healthy individuals [54,55].

Herein, for the first time, we successfully produced, purified LreCAγ, and performed a comprehensive kinetic characterization of the enzyme. In addition, we screened a panel of anions and sulfonamide derivatives (**1–24**), including clinically used drugs, to evaluate the sensitivity of the enzyme to known inhibitors. A range of amines and amino acids (**25–28**) has also been tested to identify the most effective activators of this isoform. In the second part of the study, the most promising LreCAγ activators were selected for further investigation, serving as a case study to evaluate their ability to modulate bacterial growth in a bacterial model, their anti-inflammatory potential in macrophages, and their cytocompatibility in normal intestinal epithelial cells.

2. Results and discussion

2.1. Obtainment and functional profiling of LreCAγ

2.1.1. Synthesis, cloning, expression, and production of LreCAγ

For the first time, the LreCAγ protein was successfully expressed and purified using recombinant DNA technology. The gene encoding LreCAγ was identified using a Protein BLAST search. After identification and synthesis, the gene was cloned into the pET100/D-TOPO expression vector, and the protein was heterogeneously expressed in *Escherichia coli*. After purification by affinity chromatography, approximately 90 % purity was assessed using SDS-PAGE (Fig. 1).

The enzymatic activity of LreCAγ was confirmed using the CA activity assay, by monitoring pH changes, demonstrating its ability to convert CO_2 into HCO_3^-. These results confirmed the successful expression, purification, and functional activity of the recombinant LreCAγ protein. CA was quantified in Wilbur–Anderson units, which monitored pH changes during the conversion of CO_2 to HCO_3^- at 0 °C.

2.1.2. Kinetic parameters and inhibition of LreCAγ

LreCAγ catalyzes the reversible hydration of CO_2 into HCO_3^- and H^+, similar to the slow isoform hCA I. However, its catalytic efficiency is approximately six times lower than that of the highly efficient hCA II (Table 1).

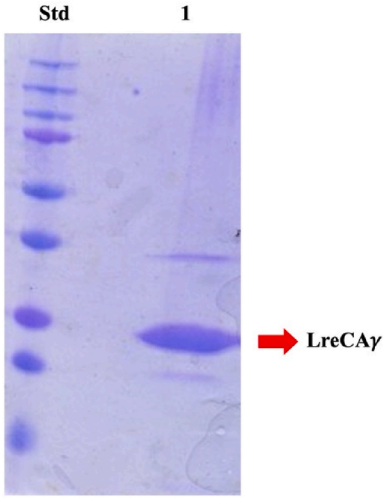

Fig. 1. SDS-PAGE analysis of purified LreCAγ. Lane Std, molecular weight markers, with bands corresponding (from top to bottom) to 250, 150, 100, 75, 50, 37, 25, 20, and 15 kDa; Lane 1, Purified recombinant LreCAγ (indicated by a red arrow) obtained after affinity chromatography. (For interpretation of the references to colour in this figure legend, the reader is referred to the Web version of this article.)

Table 1
Kinetic parameters for the CO_2-hydration reaction catalyzed by LreCAγ, along with representative α- and γ-class CA isoforms, and the inhibition constants (K_I) for acetazolamide (**AAZ**) are presented for comparative analysis.

Organism	Isozyme	Activity level	k_{cat} (s^{-1})	K_M (M)	k_{cat}/K_M (M^{-1} x s^{-1})	K_I (nM) for AAZ
H. sapiens	hCA I[a]	Moderate	2.0 × 10^5	4.0 × 10^{-3}	5.0 × 10^7	250
H. sapiens	hCA II[a]	Very high	1.4 × 10^6	9.3 × 10^{-3}	1.5 × 10^8	12
L. reuteri	LreCAγ	Moderate	2.1 × 10^5	13.4 × 10^{-3}	1.6 × 10^6	64
V. cholerae	VchCAγ[b]	Moderate	7.4 × 10^5	11.5 × 10^{-3}	6.4 × 10^7	473
E. coli	EcoCAγ[c]	Moderate	5.7 × 10^5	82.6 × 10^{-3}	6.9 × 10^6	248
P. gingivalis	PgiCAγ[d]	Moderate	4.1 × 10^5	7.5 x 10^{-3}	5.4 × 10^7	324
B. pseudomallei	BpsCAγ[e]	Moderate	5.3 × 10^5	21.2 x 10^{-3}	2.5 × 10^7	149

The cytosolic isozymes hCAs I and II (α-class), measured at 20 °C and pH 7.5 in 10 mM HEPES buffer 20 °C, and γ-CA from *L. reuteri* (LreCAγ), *V. cholerae* (VchCAγ), *E. coli* (EcoCAγ), *P. gingivalis* (PgiCAγ) and *B. pseudomallei* (BpsCAγ), measured at 20 °C and pH 8.3 in 20 mM $NaClO_4$ buffer 20 °C, are shown. Inhibition data with the clinically used sulfonamide acetazolamide (**AAZ**) are also reported for comparison purposes.
[a] Data from Supuran et al., 2008 [56];
[b] Del Prete et al., 2016 [57];
[c] Del Prete et al., 2020 [58];
[d] Ferraroni et al., 2025 [59];
[e] Vullo et al., 2017 [46].

Notably, many CAs rank among the most efficient natural catalysts, and among them, LreCAγ demonstrates significant activity. As shown in Table 1, the activity (k_{cat}) of LreCAγ is highly comparable to that of other γ isoforms, being 2- or 3-fold more active than enzymes from other bacterial organisms. However, investigating the kinetic properties of CAs is important because, even if these enzymes belong to the same family, the steric hindrance of the amino acid residues surrounding the catalytic pocket can affect parameters related to the affinity of the enzyme for the substrate (K_M).

Thus, the reference CA inhibitor acetazolamide (**AAZ**) was used as a tool for comparison across the different CAs and tested against them using the stopped-flow CO_2 hydrase assay. Interestingly, LreCAγ was inhibited by **AAZ** with an inhibition constant (K_I) in the low nanomolar range (=64 nM) (Table 1). Conversely, the compound exhibited high potency against hCA II (K_I = 12 nM) but was less effective compared to the other CAs listed in Table 1, with K_I values ranging from 149 to 473 nM. This observation could be of interest for selective CA modulator design, as the variations in K_I are associated with the different affinities of compounds for the isozymes and can be attributed to the interaction and steric hindrance of the amino acid residues in the catalytic pocket.

2.2. Inhibition of LreCAγ

To fully characterize the LreCAγ isoform, the stopped-flow-based CO_2 hydrase assay was performed to evaluate its inhibition profile using a wide selection of (in)organic anions, sulfonamides, sulfamides, and sulfamates [60].

2.2.1. Enzyme inhibition by a panel of anions

Anions represent a significant class of CA inhibitors, typically acting as coordinating ligands that interact with the metal ion in the enzyme active site. This is particularly true for CAs containing zinc ions as co-factors, with anionic compounds acting as monodentate ligands, maintaining the tetrahedral geometry of the metal center. However, in rare cases, they can adopt a trigonal bipyramidal coordination. Given their biological and pharmacological relevance, our study investigated a diverse range of organic and inorganic anions, as well as structurally related small molecules (Table 2), all known to interact with metal ions in the metalloenzyme active sites [61,62].

This study provides a comprehensive comparison between LreCAγ and VchCAγ, the latter being the most extensively characterized γ-CA isoform to date, particularly in terms of its inhibition and activation profiles [53,57]. Notably, VchCAγ shares the highest sequence and structural similarity with LreCAγ within the γ-class of CAs and originates from *V. cholerae*, a microorganism that, like *L. reuteri*, colonizes the gastrointestinal tract. Therefore, this comparison is not only of biochemical relevance but also of pharmacological interest, as it highlights the functional differences between homologous enzymes from two bacteria with contrasting roles in human health: *L. reuteri* is a beneficial probiotic and *V. cholerae* is a pathogenic species.

The data presented in Table 2 compare LreCAγ with VchCAγ and the ubiquitous hCAs I and II, revealing the following inhibition profiles.

Table 2
Inhibition data for LreCAγ by inorganic and organic anions, assessed by a stopped-flow CO_2 hydrase assay [60]. Data for hCAs I and II and a representative γ-isoform (VchCAγ) from *V. cholerae* are also reported for comparison purposes.

Cpd	K_I (mM)[a]			
	hCA I	hCA II	LreCAγ	VchCAγ[b]
F^-	>300	>300	>100	21.3
Cl^-	6	200	>100	8.8
Br^-	4	63	>100	8.7
I^-	0.3	26	>100	6.3
CNO^-	0.0007	0.03	0.57	2.6
SCN^-	0.2	1.6	0.76	13.1
CN^-	0.0005	0.02	0.45	8.4
N_3^-	0.0012	1.51	89	8.7
NO_2^-	8.4	63	22	8.7
NO_3^-	7	35	44	7.8
HCO_3^-	12	85	3.8	3.0
CO_3^{2-}	15	73	4.5	8.2
HSO_3^-	18	89	78	>200
SO_4^{2-}	63	>200	>100	9.6
HS^-	0.0006	0.04	0.93	7.9
$NH_2SO_2NH^-$	0.31	1.13	0.0030	0.084
$NH_2SO_3^-$	0.021	0.39	0.019	0.087
$PhB(OH)_2$	58.6	23	0.033	0.081
$PhAsO_3H^-$	31.7	49	0.046	0.091
ClO_4^-	>200	>200	>100	>200
SnO_3^{2-}	0.57	0.83	5.1	2.9
SeO_4^{2-}	118	112	58	9.1
TeO_4^{2-}	0.66	0.92	1.9	7.2
OsO_5^{2-}	0.92	0.95	9.0	NA
$P_2O_7^{2-}$	25.8	48	69	7.3
$V_2O_7^{2-}$	0.54	0.57	7.3	8.3
$B_4O_7^{2-}$	0.64	0.95	2.9	7.2
ReO_4^-	0.11	0.75	4.4	>200
RuO_4^-	0.101	0.69	7.3	>200
$S_2O_8^{2-}$	0.107	0.084	76	>200
$SeCN^-$	0.085	0.086	0.87	8.7
$NH(SO_3)_2^{2-}$	0.31	0.76	2.8	8.1
FSO_3^-	0.79	0.46	84	7.5
CS_3^{2-}	0.0087	0.0088	6.7	8.8
$EtNCS_2^-$	0.00079	0.0031	0.65	0.44
PF_6^-	>50	>50	>100	>200
$CF_3SO_3^-$	>50	>50	8.1	>200

[a] Mean from three different assays, by a stopped-flow technique with errors in the range of ± 5–10 % of the reported values.
[b] Data from Del Prete et al., 2016 [57].

i. Halides, sulfate, perchlorate, and hexafluorophosphate did not inhibit LreCAγ at concentrations up to 100 mM. Notably, halides inhibited hCA I and VchCAγ in the low millimolar range (with the exception of fluoride in hCA I) but exhibited weaker inhibition against hCA II. In contrast, sulfate acted as a potent inhibitor of VchCAγ and a weaker inhibitor of hCA I.

ii. Weak inhibition of LreCAγ was observed for nitrite, nitrate, hydrogen sulfite, selenate, pyrophosphate, and fluorosulfonate, with inhibition constants (K_Is) ranging from 21 to 84 mM. Surprisingly, azide, which typically shows a high affinity for cations, was the weakest inhibitor in this subset (K_I = 89 mM). Conversely, all these anions inhibited VchCAγ in the low millimolar range, except for hydrogen sulfite, which was inactive. Interestingly, azide, pyrophosphate, and fluorosulfonate act as sub-millimolar or low-millimolar inhibitors of hCA I and II.

iii. Significant inhibition of LreCAγ was observed for bicarbonate, carbonate, stannate, tellurate, osmate, divanadate, tetraborate, perrhenate, perruthenate, iminodisulfonate, trithiocarbonate, and triflate, which presented K_I values in the range of 1.9–9.0 mM. Again, a similar trend was observed for VchCAγ, except for perrhenate and perruthenate, which were inactive. Instead, all these anions generally function as micromolar inhibitors of hCA I and II, except for bicarbonate, carbonate, and triflate, which more effectively inhibit LreCAγ.

iv. The most potent inhibitors of LreCAγ were isocyanate, isothiocyanate, cyanide, hydrogen sulfide, selenocyanide, and *N*,*N*-diethyldithiocarbamate, with K_I values between 0.45 and 0.87 mM. All these anions inhibited LreCAγ more potently than VchCAγ. In particular, the most effective LreCAγ inhibitors were sulfamide, sulphamic acid, phenyl arsenic acid, and phenylboronic acid, with K_Is of 3, 19, 33, and 46 μM, respectively. This inhibition profile is consistent with that of hCA I and II, except for phenylarsenic and phenylboronic acids, which are weaker inhibitors of human isoforms.

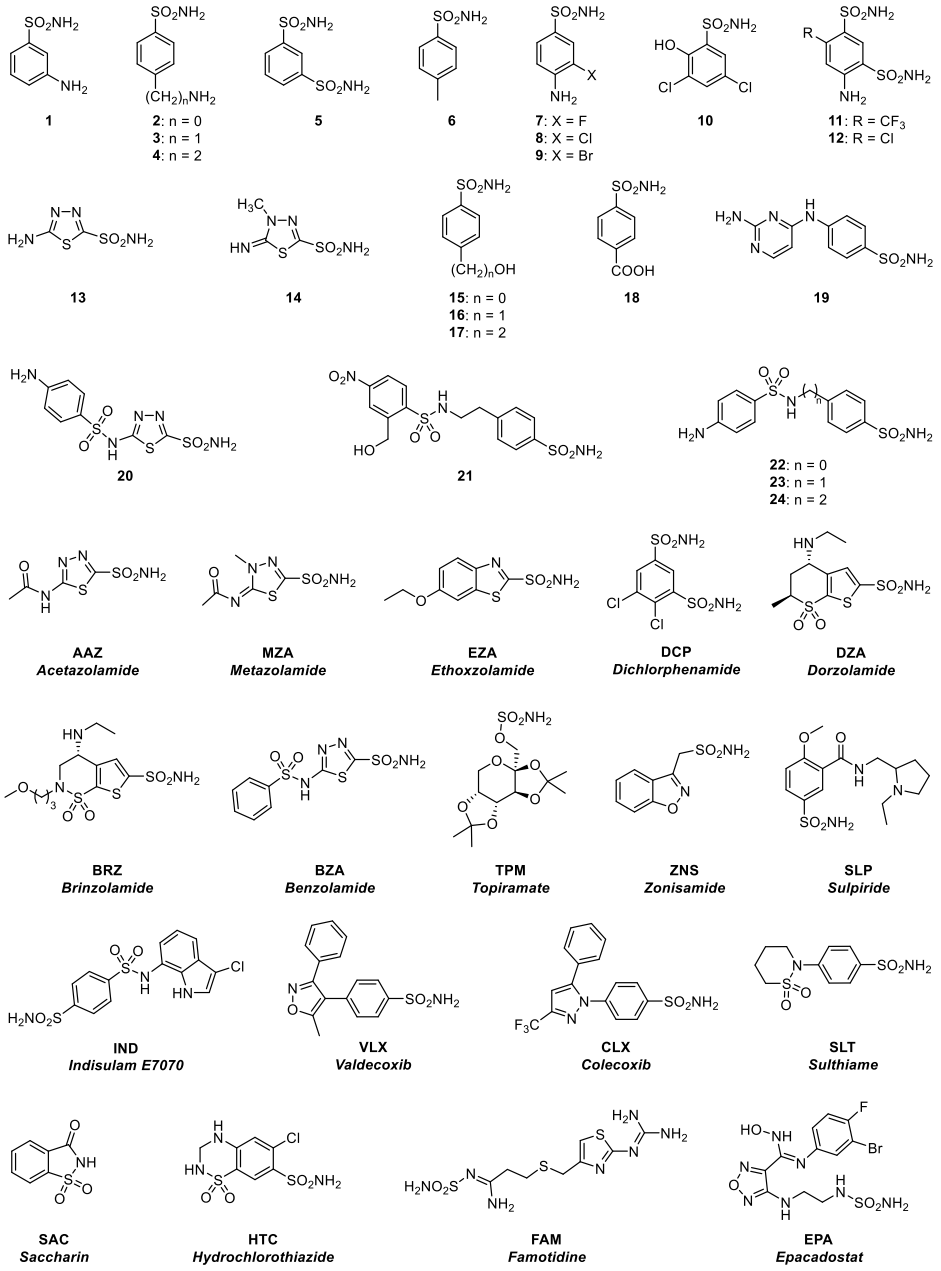

Fig. 2. Commercial and clinical sulfonamides/sulfamates/sulfamides investigated as LreCAγ inhibitors.

Distinct differences in the inhibition profiles of bacterial and human CAs in response to inorganic and organic anions were found, suggesting potential elements for designing tools to selectively target bacterial enzymes, without perturbing host homeostasis. Furthermore, some interesting insights can be extrapolated if we consider the results for LreCAγ and VchCAγ, where the various anions tested showed different inhibition profiles against these isoforms. This could be a starting point for understanding how the development of selective inhibitors can selectively modulate the growth of microorganisms that share the same host district.

2.2.2. Enzyme inhibition by a panel of sulfonamides and related compounds

The chemical structures of the commercial (**1-24**) and clinically used (**AAZ-EPA**) sulfonamides, sulfamides, and sulfamates tested in the inhibition studies on LreCAγ are presented in Fig. 2, and the K_I values are reported in Table 3, with hCAs I and II and VchCAγ reported for comparison.

Overall, these compounds inhibit hCA II > LreCAγ = VchCAγ > hCA I, in that order, being LreCAγ inhibitors in the range of 64.3–7914 nM. Concerning the inhibition data in Table 3, the following trends were observed.

i. Among the tested sulfonamides, **SAC** was the weakest LreCAγ inhibitor (K_I = 7900 nM), with approximately a 2-fold stronger inhibition profile with respect to hCA I.
ii. Compounds **2–4**, **7**, **10–12**, **19**, **23**, **DCP**, **BRZ**, **BZA**, **TPM**, **SLP**, **VLX**, **CLX**, **HTC**, **FAM**, and **EPA** inhibited LreCAγ with K_I values between 130 and 990 nM. Among these, derivatives **3**, **19**, **BZA**, and **HTC** exhibited weaker inhibition of LreCAγ than the human CA isoforms. Instead, VchCAγ was inhibited by **2–4**, **7**, **11**, **BRZ**, **BZA**, **TPM**, and **SLP** with K_I values below 100 nM. On the other hand, sulfonamides **12**, **19**, **23**, **DCP**, **VLX**, and **CLX** were weaker inhibitors of VchCAγ than LreCAγ. This finding is especially noteworthy as it may expand the factors influencing a physician's selection of clinical sulfonamides, facilitating the development of the most suitable therapy for the patient while maintaining the balance of commensal bacteria in the microbiota.
iii. A good inhibition profile in the range of 64–97 nM was observed for sulfonamides **1**, **5**, **6**, **8**, **9**, **13–18**, **20–22**, **24**, **AAZ**, **MZA**, **EZA**, **DZA**, **ZNS**, **IND**, and **SLT.** While sulfonamides **5**, **6**, **8**, **9**, **13–15**, **24**, **MZA**, **EZA**, **DZA**, and **IND** showed similar inhibitory activity against VchCAγ, derivatives **1**, **16–18**, **20–22**, **AAZ**, **ZNS**, and **SLT** were more potent and selective inhibitors of LreCAγ. Notably, compounds **1**, **5**, **6**, **8**, and **17** emerged as the most selective LreCAγ inhibitors with respect to both hCA I and II, with selectivity ratios ranging from 118 to 312 over hCA I and 1.3–3.2 for hCA II. Considering the experimental errors (±5–10 %), the K_I values for derivatives **15** and **16** against LreCAγ and hCA II are comparable. Among these, compounds **1** and **17** were the most selective LreCAγ inhibitors with respect to VchCAγ, with selectivity ratios of 7.3 and 92.88, respectively.
iv. Rationalizing the structure-activity relationships (SARs) in this case is challenging due to the structural diversity of the tested sulfonamides, which include both aromatic (benzenesulfonamides) and heterocyclic derivatives. However, certain trends emerged: *m*-substituted aromatic sulfonamides generally exhibited stronger inhibitory activity than *p*-substituted ones (*e.g.*, compounds **1** and **5** compared to **2–4**) against LreCAγ, while the introduction of bulkier substituents tended to reduce potency (*e.g.*, in **5** and **DZA** compared to **DCP** and **BRZ**). Additionally, heteroaromatic sulfonamides often exhibit greater inhibitory activity than their benzene counterparts (*e.g.*, compounds **13**, **14**, and **20** compared to **2** and **22–24**, or **AAZ**, **MZA**, **EZA**, **DZA**, **BRZ**, and **BZA** show higher potency than **DCP**, **SLP**, **VLX**, and **CLX**). Once again, the secondary sulfonamide **SAC** exhibited the weakest inhibition profile among all the tested compounds. In the case of sulfonamides, structural diversity is a key determinant of selectivity. Aromatic derivatives with meta-substitutions generally show stronger inhibition of LreCAγ compared to para-substitutions, which can be rationalized by improved accommodation within the enzyme active site. Likewise, heteroaromatic sulfonamides frequently outperform their benzene analogues, suggesting that heteroatoms facilitate additional polar interactions with the enzyme. Our findings underscore how subtle structural variations of inhibitors and activators can be exploited to achieve isoform selectivity. This has important implications for the rational design of modulators that could enhance probiotic functionality via LreCAγ without affecting host or pathogenic CAs.

Table 3
Inhibition data for LreCAγ by sulfonamides/sulfamates/sulfamides **1–24** and the clinically used drugs (**AAZ-EPA**), assessed by a stopped-flow CO_2 hydrase assay [60]. Data for hCAs I and II and a representative γ-isoform (VchCAγ) are also reported for comparison purposes.

Cpd	K_I (nM)[a]			
	hCA I	hCA II	LreCAγ	VchCAγ
1	28000	300	92	672
2	25000	240	400	95
3	79	8.0	530	81
4	78500	320	700	69
5	25000	170	86	94
6	21000	160	75	76
7	8300	60	130	73
8	9800	110	83	73
9	6500	40	97	95
10	7300	54	550	544
11	5800	63	330	87
12	8400	75	160	563
13	8600	60	92	66
14	9300	19	97	70
15	5500	80	69	88
16	9500	94	91	556
17	21000	125	67	6223
18	164	46	87	5100
19	109	33	190	4153
20	6.0	2.0	65	5570
21	69	11	90	764
22	164	46	79	902
23	109	33	130	273
24	95	30	94	73
AAZ	250	12	64	473
MZA	50	14	75	494
EZA	25	8.0	86	85
DCP	1200	38	820	1230
DZA	50000	9.0	93	87
BRZ	45000	3.0	170	93
BZA	15	9.0	310	78
TPM	250	10	210	69
ZNS	56	35	92	725
SLP	1200	40	250	78
IND	31	15	92	91
VLX	54000	43	380	817
CLX	50000	21	370	834
SLT	374	9.0	86	464
SAC	18540	5959	7900	550
HTC	328	290	790	500
FAM	922	58	950	>100000
EPA	8262	917	990	>100000

[a]Mean from three different assays, by a stopped-flow technique (errors were in the range of ± 5–10 % of the reported values).
[b]Data from Del Prete et al., 2016 [57].

2.3. Activation of LreCAγ

The activation of LreCAγ holds significant therapeutic potential for supporting probiotics that help restore a balanced gut microbiota or for

utilizing *L. reuteri* as a resource competitor to counteract bacterial infections in the gastrointestinal tract. Identifying new probiotic-stimulating agents is a promising strategy for maintaining a healthy microbiota, thereby contributing to the prevention and treatment of pathological conditions in humans. In addition, some of these compounds are components of bacterial growth media, metabolites that can arrive in the gut, or signalling compounds between the host and microbiota (produced and secreted by both).

2.3.1. Enzyme activation by a panel of amines

In this context, a wide panel of amines, including amino acids, both natural (*L*) and non-natural (*D*) (Fig. 3), were tested on LreCAγ, and in Table 4, the activation constants (K_A), compared with those for VchCAγ, hCA I and II, are reported.

Although all tested compounds exhibited a similar activation profile of LreCAγ within the range of 8.3–37.2 μM, which is generally weaker than that observed for VchCAγ, the following considerations can be made.

i. Derivatives **27**, **29**, **30**, **33–35**, **37**, and **39–42** showed a weaker activation profile for LreCAγ than hCA I and II, with K_As ranging from 10.2 to 37.2 μM.
ii. Compounds **25**, **26**, **36**, and **43–47** activated hCA I > LreCAγ > hCA II, in that order, whereas amino acids **28** and **32** activated VchCAγ > hCA II > LreCAγ > hCA I, respectively. Among these, derivatives **25** and **26** emerged as the most potent LreCAγ activators, with K_A values of 8.3 and 9.7 μM, respectively. Again, compound **26** was the only selective activator of LreCAγ compared to VchCAγ.
iii. A selective activation profile for LreCAγ was observed with activators **31**, **38**, and **48**, compared to human isoforms, with selectivity ratios ranging from 1.7 up to more than 6.4-fold relative to hCA I and from 1.6 to >3.2-fold relative to hCA II.

Generally, both amines and amino acids exhibited a similar activation trend, and stereochemistry did not play a crucial role in activity, as both *L*- and *D*-amino acids demonstrated comparable activation levels. The only exception was *L*-Phe (**27**), which proved to be 2-fold more potent than *D*-Phe (**28**). This case also provides noteworthy insights.

Table 4
Activation data for LreCAγ by amines and amino acids **25**–**48**, assessed by a stopped-flow CO_2 hydrase assay [60]. Data for hCAs I and II, and a representative bacterial γ-isoform (VchCAγ) are also reported for comparison purposes.

Cpd		K_A (μM)[a]			
		hCA I	hCA II	LreCAγ	VchCAγ[b]
25	*L*-His	0.03	10.9	8.3	1.01
26	*D*-His	0.09	43	9.7	14.2
27	*L*-Phe	0.07	0.013	10	0.73
28	*D*-Phe	86	0.035	25	0.24
29	*l*-DOPA	3.1	11.4	25	0.19
30	*d*-DOPA	4.9	7.8	32	0.13
31	*L*-Trp	44	27	16	0.008
32	*D*-Trp	41	12	14	0.40
33	*L*-Tyr	0.02	0.011	33	0.12
34	*D*-Tyr	0.04	0.013	34	0.10
35	*L*-Phe-(4-NH_2)-OH	0.24	0.15	33	0.69
36	Histamine	2.1	125	25	0.31
37	Dopamine	13.5	9.2	31	0.45
38	Serotonin	45	50	26	0.17
39	2-Pyridyl-methylamine	26	34	37	0.14
40	2-(2-Aminoethyl) pyridine	13	15	31	0.26
41	1-(2-Aminoethyl)-piperazine	7.4	2.3	25	0.0071
42	4-(2-Aminoethyl)-morpholine	0.19	0.94	13	>100
43	*l*-Adrenaline	0.09	96	33	>100
44	*L*-Asn	11.3	>100	25	>100
45	*L*-Asp	5.2	>100	32	>100
46	*L*-Glu	6.43	>100	30	>100
47	*D*-Glu	10.7	>100	30	>100
48	*L*-Gln	>100	>50	16	>100

[a] Mean from three different assays, by a stopped-flow technique (errors were in the range of ± 5–10 % of the reported values).
[b] Data from Angeli et al., 2018 [53].

Similar to inhibitors, activators exhibit distinct activation profiles depending on the specific CA isoform, a variability that can be attributed to differences in the amino acid composition of their active sites. These structural variations enable diverse modes of interaction with activating compounds. Consequently, it is feasible to design isoform-selective activators of LreCAγ to promote the performance of this probiotic, offering

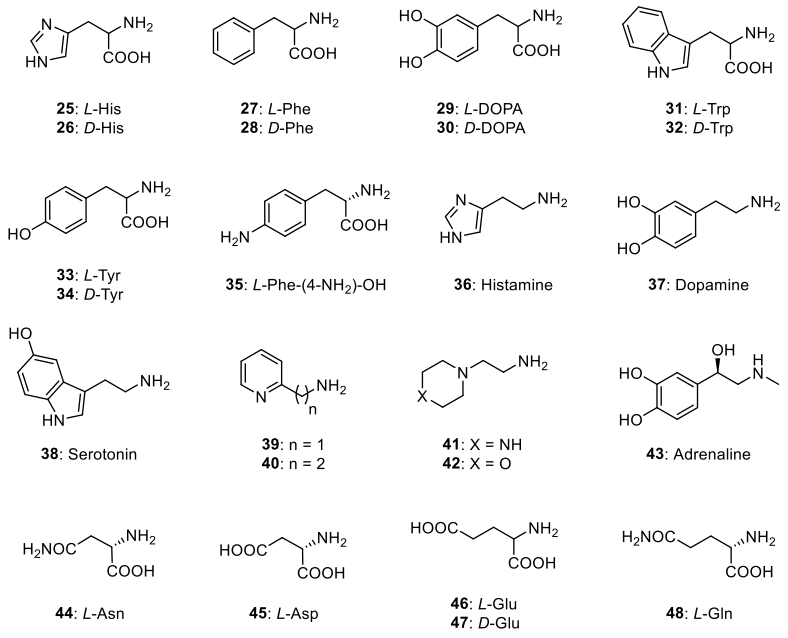

Fig. 3. Structure of amino acids and amines (activators panel) investigated as LrCAγ activators.

a potential strategy to selectively treat dysbiosis, without disrupting the growth of other pathogenic or non-pathogenic intestinal microorganisms.

2.4. Structural insight into LreCAγ

Structural insights are crucial for elucidating the catalytic mechanism of the LreCAγ, and following an initial crystallization screen, two different crystal forms were obtained for LreCAγ. From the data collected on the first crystal form, belonging to the orthorhombic space group *I*222, we solved and refined the structure at 2.80 Å resolution. These crystals were obtained using a precipitant solution containing 0.2 M magnesium formate dihydrate and 20 % (w/v) PEG 3350. The second crystal form was obtained from conditions containing 2.0 M ammonium sulfate, 0.1 M HEPES pH 7.5, and 2 % (v/v) PEG 400, yielding crystals in the orthorhombic space group $P2_12_12_1$. Diffraction data collected on these crystals extended to atomic resolution (1.26 Å). Both crystal forms contained three monomers per asymmetric unit. Data collection parameters and refinement statistics are summarized in Table S1.

The structures were solved by molecular replacement, using the AlphaFold-predicted model as the initial template. Electron density maps showed clear definition for all 179 amino acids except for the first N-terminal residue in each monomer, which we introduced with occupancy equal to in the refined model. Structural superposition of the experimental and predicted models revealed a close overlap (R.M.S.D. of 0.364), with no major global deviations between the alphafold model and the structure at 1.26 Å (Fig. 4). On the other hand, the structure at 2.8 Å showed a variability in the orientation of the so-called acid loop, as highlighted in Fig. 4, probably due to a different crystal packaging inside the crystal lattice.

Since no substantial structural differences were observed between the two experimental models, the high-resolution structure is described here in detail. LreCAγ forms a trimer of identical monomers, each adopting the characteristic seven-turn left-handed β-helix fold capped by a C-terminal α-helix that runs antiparallel to the β-helix axis, consistent with previous X-ray structural studies on γ-CAs (Fig. 5A) [63–67].

The trimeric assembly showed three active sites located at the interfaces between adjacent monomers, and a zinc ion was coordinated by three histidine residues in a tetrahedral geometry (His67 and His96 from one monomer and His91 from the neighbouring subunit) together with a water molecule (W1). This differs from the structure of the prototype γ-CA, Cam, in which the zinc ion is coordinated by two water molecules [67]. In LreCAγ, W1 is stabilized through hydrogen bonding with Tyr159, functioning analogously to the gatekeeper Thr199 in α-CAs and Asn202 in Cam [67], thereby positioning the hydroxide ion for nucleophilic attack on the CO_2 substrate (Fig. 5B). In addition to W1, two further water molecules (W2 and W3) are located within the active site, forming an extended hydrogen-bonding network with surrounding residues, suggesting a potential role in the catalytic process (Fig. 5B). Several residues, crucial for trimer stabilization and active-site integrity as Arg46, Asp48, and Asp62 (corresponding to Arg59, Asp76, and Asp61 in Cam), are conserved in LreCAγ, as in other γ-CAs reported previously [59,67,68]. Notably, Glu84, which functions as a proton shuttle in Cam (analogously to His64 in hCA II), is replaced by Arg70 in LreCAγ. This substitution, which is not universally conserved among catalytically active γ-CAs, suggests variability in the positioning of the proton shuttle residue within the family, potentially contributing to differences in catalytic efficiency. Interestingly, in one active site, a sulfate anion was observed bound directly to Zn^{2+}, displacing W1 and generating a distorted trigonal bipyramidal coordination environment (Fig. 5C). Although sulfate did not inhibit LreCAγ at tested concentrations (K_I > 100 μM), this binding mode resembles that of an inhibitor, with one oxygen atom forming a hydrogen bond with the side chain of Tyr168.

When comparing the three-dimensional structure of LreCAγ with those of Cam, PgiCAγ and BpsCAγ [59,67,68],it becomes evident that although all share the characteristic left-handed β-helix fold capped by a C-terminal α-helix, variations are present in the regions preceding the α-helix and in several loop segments (Fig. 6).

Among the four homologous enzymes, Cam is unique in containing a short α-helix connecting the β-helix to the C-terminal α-helix. In contrast, LreCAγ, BpsCAγ, and PgiCAγ display a β-strand in this position, resulting in a distinct orientation of the initial C-terminal α-helix in Cam compared with the other γ-CAs. The most pronounced structural

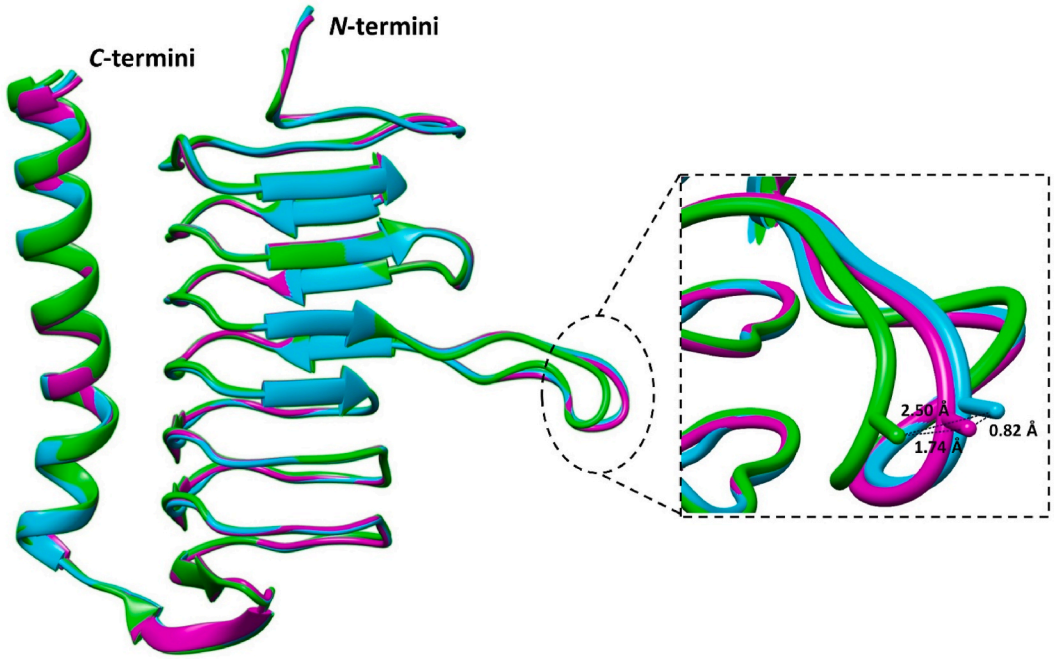

Fig. 4. Superposition of the predicted AlphaFold LreCAγ structure (cyan) with the experimental LreCAγ structures, in magenta (PDB: 9SUZ) at 1.26 Å of resolution and in green (PDB: 9SUT) at 2.80 Å of resolution. Zoomed view illustrates the positional differences of the "acid loop". (For interpretation of the references to colour in this figure legend, the reader is referred to the Web version of this article.)

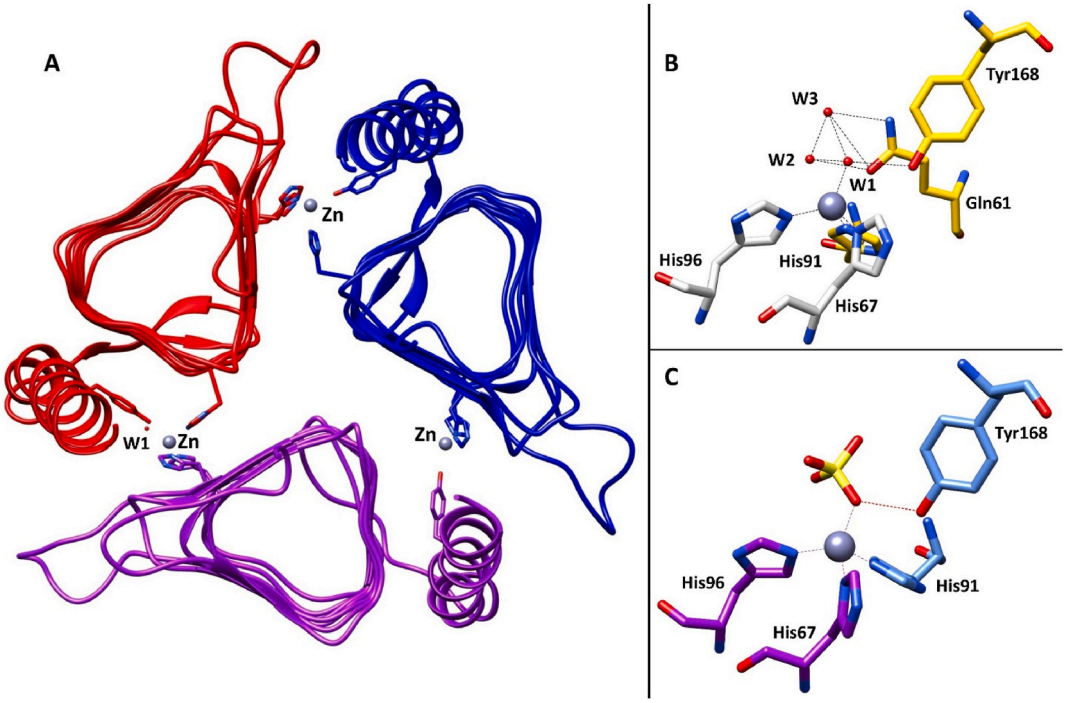

Fig. 5. A) The LreCAγ trimer, with the three monomers shown in purple, red, and blue, respectively. The zinc ions are also depicted. **B)** Active site region of LreCAγ. Residues from one subunit are coloured in light grey and residues from a second subunit in yellow. Dotted lines represent the zinc ion coordination and red dotted lines hydrogen bonds. **C)** Active site region of LreCAγ with the SO_4^{2-} inhibitor bound. Residues from one subunit are coloured in purple and residues from a second subunit in blue with dotted lines representing zinc coordination and hydrogen bonds, as previously indicated. (For interpretation of the references to colour in this figure legend, the reader is referred to the Web version of this article.)

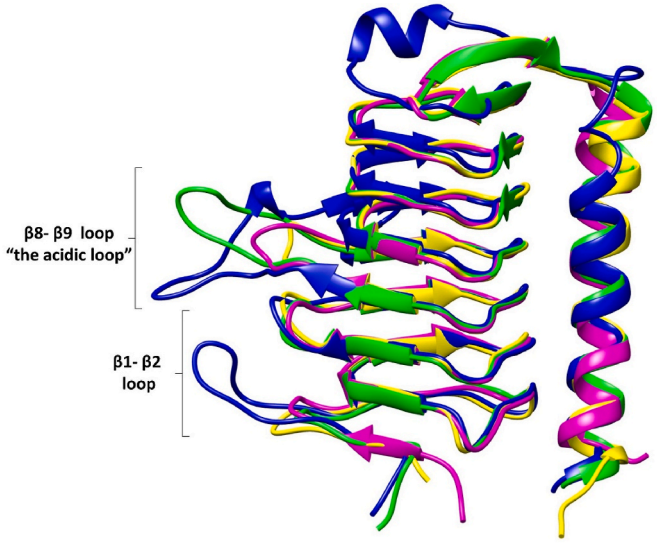

Fig. 6. Structural superposition of LreCAγ (green, PDB: 9SUZ), Cam (blue, PDB: 1QRG), PgiCAγ (magenta, PDB: 9GVA), and BpsCA γ (yellow, PDB: 7ZW9). (For interpretation of the references to colour in this figure legend, the reader is referred to the Web version of this article.)

differences are located in two regions: the β1–β2 loop and the β8–β9 loop. In the β1–β2 loop, all isoforms except Cam adopt a similar conformation, whereas Cam features an elongated loop that extends to pack against the neighbouring protomer within the trimer [67]. In the β8–β9 loop, also referred to as the "acidic loop", even greater variability is observed. Cam and LreCAγ both possess an extended loop, while PgiCAγ and BpsCAγ exhibit shorter counterparts (Fig. 6).

2.5. Effects of selected CA activators on E. coli growth

To investigate the role of CA modulators in bacterial growth, we developed an *ad hoc* assay using *E. coli* cultures [69]. *E. coli* DH5α was chosen as a reference model for Gram-negative bacteria because it is easy to cultivate and grows rapidly under standard laboratory conditions. Regarding CA expression, *E. coli* encodes several CAs, specifically CynT and CynT2, both belonging to the β-class, YadF, also known as EcoCAγ, and an ι-CA. EcoCAβ (CynT2) and EcoCAγ have previously been isolated and characterized by our group, and their enzymatic activity has been thoroughly profiled [58,70,71]. Among these, CynT2 is essential for the growth of the microorganism at atmospheric pCO_2 [72,73], making it the physiologically relevant isoform for assessing the impact of CA activators on proliferation. Although EcoCAγ and ι-CA are encoded in the genome, their contribution under these conditions is negligible. Therefore, the activation profiles were determined exclusively for EcoCAβ, providing meaningful insights into the CA-dependent effects observed in our assays.

The designed assay involves testing selected CA activators alone or in combination with **AAZ**, as a reference CA inhibitor. The rationale behind this approach is to assess whether certain amines, potentially acting as growth enhancers for *E. coli*, exert their effects through CA activation. Co-treatment with **AAZ** is used to selectively suppress CA activity, thereby allowing us to determine whether the observed compound-caused growth effects are CA-dependent. Briefly, **AAZ** was used in the assays at a concentration of 1.0 mg/mL (4.5 μM), as previous studies showed an effect on cell growth at this level (green bars, Fig. 7), whereas complete growth inhibition was observed at 4.0 mg/mL [62].

CA activators (Fig. 3) were selected based on their chemical structure, stereochemistry, activation potency, and isoform selectivity toward EcoCAβ (data have already been published) [58,70,71]. Specifically, kinetics studies on EcoCAβ (Fig. 7) revealed varying K_A values among the tested amines, with serotonin (**38**) exhibiting the highest potency ($K_A = 2.76$ μM), followed by L-Phe-(4-NH_2)-OH (**35**, K_A

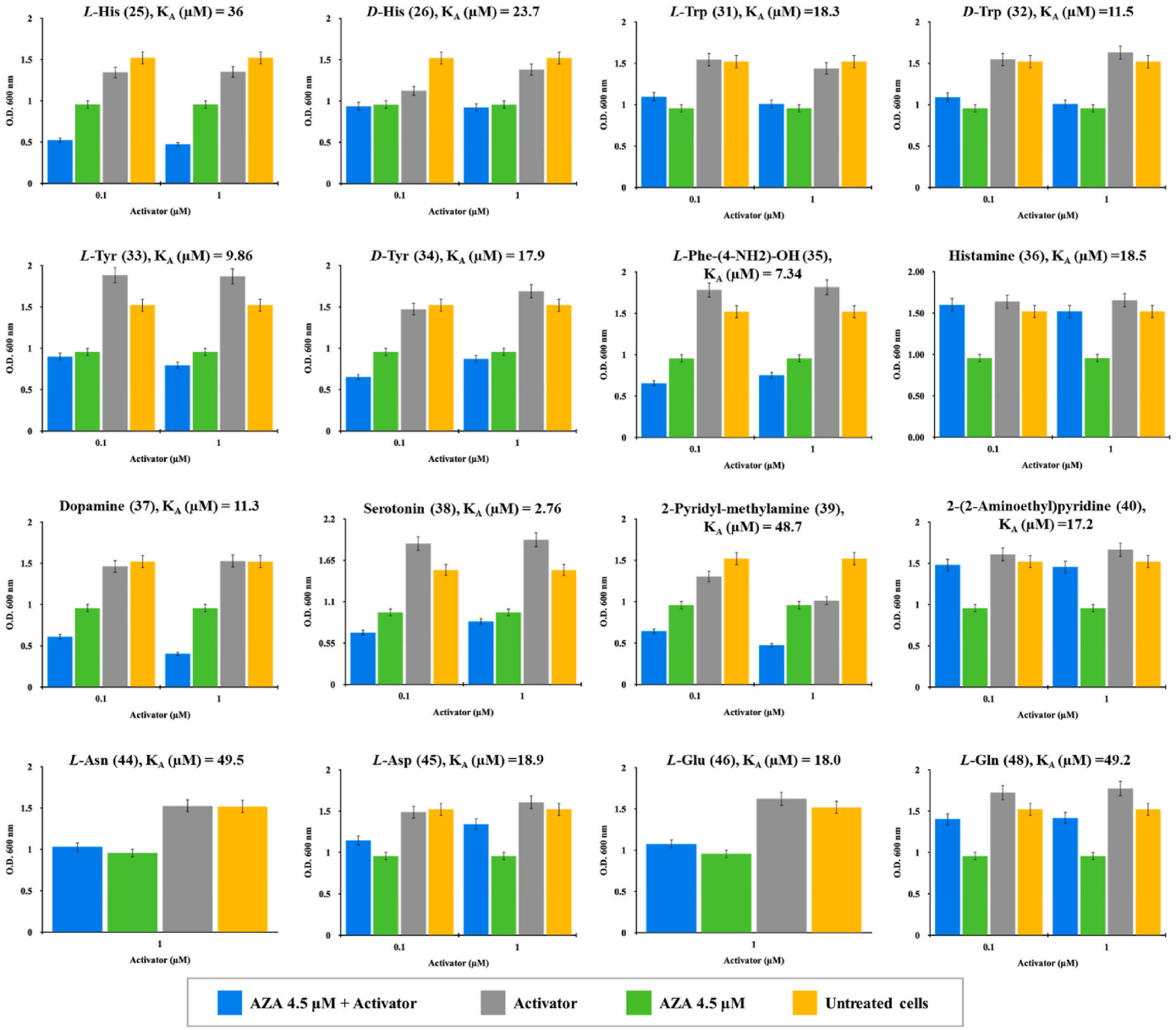

Fig. 7. Effect of CA activators and **AAZ** on *E. coli* DH5α growth. *E. coli* cells were treated with selected CA activators at concentrations of 0.1 and 1.0 μM while evaluating their modulatory effects on bacterial proliferation. Among the activators, L-Glu (**46**) and L-Asn (**44**) were tested only at 1.0 μM. **AAZ** was added at a fixed concentration of 4.5 μM, and its combination with each activator was also tested to determine potential interactions affecting bacterial growth. Growth was monitored spectrophotometrically by measuring optical density at 600 nm (OD_{600}) over time. For each activator, the K_A value is reported for EcoCAβ. Data are expressed as mean ± SD from three independent experiments, each performed in triplicate.

= 7.34 μM), L-Tyr (**33**, K_A = 9.86 μM), and dopamine (**37**, K_A = 11.3 μM). Whereas L-His (**25**, K_A = 36 μM) and L-Asn (**44**, K_A = 49.5 μM) displayed relatively weaker activation effects.

Interestingly, the assays demonstrated that the activators influenced bacterial proliferation in a concentration-dependent manner (Fig. 7). In fact, the optical density (OD_{600}) measurements of *E. coli* cultures treated with the selected CA activators **25**, **33**, **35**, **37**, **38**, and **44** indicated that L-Tyr (**33**), D-Tyr (**34**), L-Phe-(4-NH_2)-OH (**35**), and serotonin (**38**) promoted bacterial cell growth, as shown by the increase in OD_{600} values (grey bars, Fig. 7) compared to the untreated control (yellow bars, Fig. 7). The presence of **AAZ** (green bars) led to a notable reduction in *E. coli* growth, which confirmed its inhibitory effect on EcoCAs activity. This decline in OD_{600} values was observed across all experimental conditions, indicating that inhibition of β-CA negatively impacts bacterial proliferation. When Histamine (**36**), 2-(2-aminoethyl)pyridine (**40**), L-Asp (**45**), and L-Gln (**48**) were co-administered with **AAZ** (blue bars, Fig. 7), bacterial growth was partly restored compared to treatment with AAZ alone. In contrast, compounds such as L-Glu (**46**), L-Asn (**44**), L-Trp (**31**), and D-Trp (**32**) produced no significant change under co-treatment, suggesting only a weak interplay between their limited activation and AAZ inhibition. For the remaining activators, the presence of **AAZ** resulted in an increased inhibitory effect on bacterial growth. The combination of CA activator and AAZ may likely create a competing balance in terms of enzyme regulation, where the activators push for increased EcoCAβ activity, whereas **AAZ** suppresses this activity. The outcome of this balance would naturally result in a decrease in optical density if the inhibitor effect outweighed the activator influence. Although these assays in *E. coli* provide valuable mechanistic insights into CA-dependent growth modulation, they do not substitute for experiments in *L. reuteri*. Thus, the observed effects should be regarded

as an indirect model, and extrapolation to the probiotic strain must await future validation.

2.6. Effects of selected CA activators on human macrophages and human intestinal epithelial cells

The biological effect of selected CA activators was afterwards evaluated on human macrophages under basal and pro-inflammatory conditions after 24 h of exposure, and on an epithelial cell line isolated from the small intestine (HIEC-6) after 24 h and 48 h of exposure (Fig. 8).

CA activators, which underwent biological evaluations (**25**, **26**, **31**, **32**, **38**, and **48**), were selected on the basis of potency, stereochemistry, and isoform selectivity. Under basal conditions (Fig. 8a), the cell metabolic activity of macrophages is not significantly modulated, with the exception of compound **38**, which stimulates macrophage metabolism in a dose-dependent manner. As expected, the stimulation with lipopolysaccharide (LPS) alone dramatically increases the cell metabolic activity of macrophages, as a sign of immunostimulation. Compounds **31** and **32** are the most effective ones capable of counteracting the cell metabolic activity trend triggered by LPS, leading to values that are comparable to the untreated sample (Fig. 8b). In parallel, only L-Trp (**31**) shows a good biocompatibility on HIEC 6 cells at all the concentrations tested (Fig. 8c), while **25**, **26**, **38**, and **48** significantly decrease cell metabolic activity only at the lowest concentration tested. Finally, compound **32** lowers the percentage of metabolically active intestinal cells in a dose-dependent manner.

The consistent, dose-dependent effects of CA activators on both bacterial growth and macrophage responses, together with the comprehensive biochemical characterization of LreCAγ, provide strong mechanistic evidence for its functional role. Although direct genetic manipulation was not undertaken, the reproducibility and specificity of these responses provide substantial support for the involvement of LreCAγ.

3. Conclusions

In summary, we reported, for the first time, the recombinant production, isolation, purification, and functional characterization of the γ-class CA from the probiotic bacterium *L. reuteri*, named LreCAγ. The successful expression and kinetic profiling of LreCAγ represent a novel contribution to the understanding of probiotic enzymes, providing a foundation for further biochemical and pharmacological investigations. Herein, we performed and discussed a comprehensive, systematic evaluation of panels of canonical CA modulators, such as inhibitors with inorganic and organic anionic nature, sulfonamide and related structures, along with amines and amino acids. The differential inhibition and activation profiles observed between LreCAγ and both hCAs I and II and VchCAγ highlight the feasibility of designing isoform-selective modulators, which could enhance probiotic activity without adversely affecting the host or pathogenic CAs. Interestingly, among the activators tested, some compounds demonstrated the ability to stimulate bacterial growth in *E. coli,* probably through a CA-dependent mechanism, and modulate inflammatory responses in human macrophages, with L-Trp (**31**) showing particularly promising biocompatibility in intestinal epithelial cells. These findings provide proof-of-concept that LreCAγ activity can modulate bacterial growth and immune responses. While formal causality has yet to be established, the convergence of biochemical, pharmacological, and phenotypic evidence robustly supports the functional relevance of LreCAγ, underscoring its potential as a

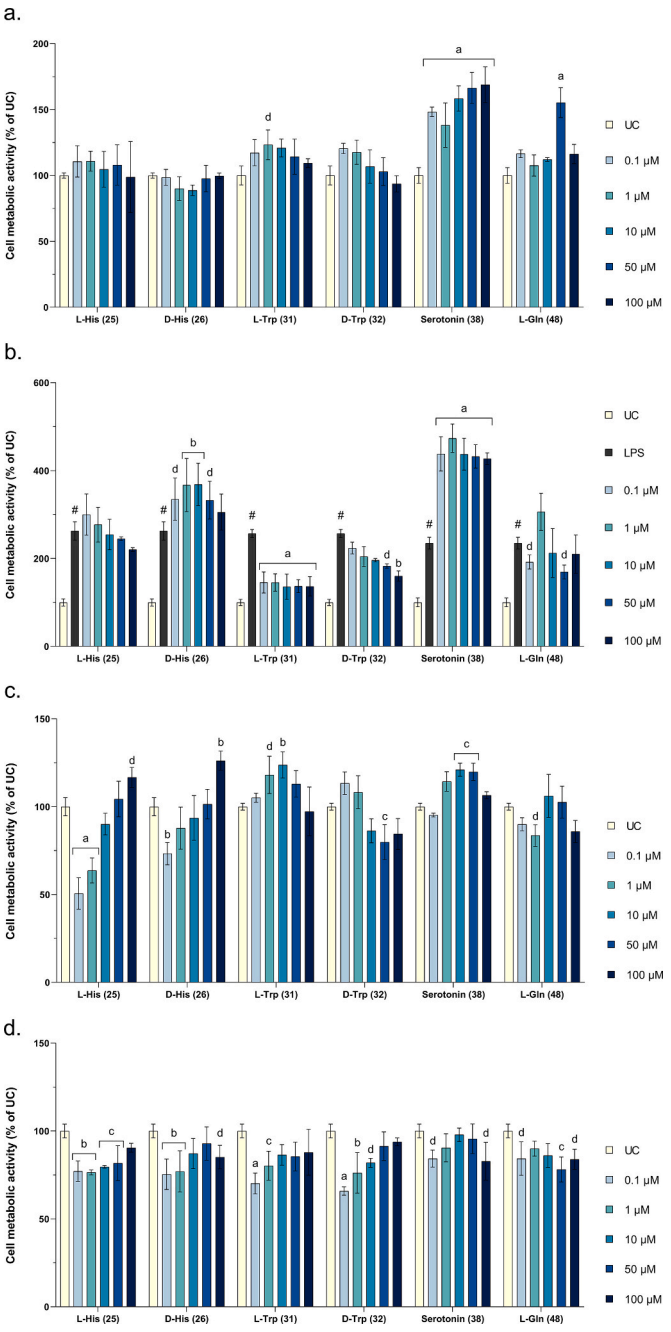

Fig. 8. Cell metabolic activity of: (**a**) human differentiated macrophages under basal conditions after 24 h of exposure; (**b**) LPS-stimulated human differentiated macrophages after 24 h of exposure; (**c-d**) human intestinal epithelial cells HIEC-6 after 24 h and 48 h of exposure. Cells were treated with compounds **25**, **26**, **31**, **32**, **38**, and **48**, administered at 0.1, 1, 10, 50, and 100 μM. Metabolic activity of untreated cells (UC) was set at 100 %. Data are presented as mean ± standard deviation (SD). Each experiment was performed twice in triplicate per experimental condition (n = 6). a = $p < 0.0001$, b = $p < 0.0010$, c = $p < 0.0050$, and d = $p < 0.0250$ comparing treated cells to the untreated cells; # = $p < 0.0001$ comparing LPS-stimulated cells to untreated cells.

target for modulating probiotic functionality. These results collectively support the feasibility of targeting LreCAγ as a novel concept to modulate probiotic functionality. However, it is important to emphasize that the bacterial growth assays were performed in *E. coli* as a surrogate model, and the effects on *L. reuteri* itself remain to be directly validated. Therefore, while our findings provide a proof-of-concept, further dedicated studies on *L. reuteri* cultures will be essential before firm translational conclusions can be drawn regarding probiotic enhancement.

4. Experimental section

4.1. Cloning, expression, and purification of the recombinant LreCAγ

4.1.1. Chemicals and instruments

The materials and instruments used in this study were obtained from various sources. Isopropyl β-D-1-thiogalactopyranoside (IPTG) and antibiotics were purchased from Merck (Darmstadt, Germany). His-Trap FF affinity column and molecular weight markers were sourced from Cytiva (Uppsala, Sweden). Additional equipment included the AKTA Prime purification system (Cytiva), SX20 Stopped-Flow instrument (Applied Photophysics, Leatherhead, UK), iBright 1500 Imaging System (Thermo Scientific, Waltham, MA, USA), and SDS-PAGE apparatus (Bio-Rad, Hercules, CA, USA). Unless otherwise stated, all other reagents were of analytical grade.

4.1.2. Gene identification, synthesis, cloning, and heterologous expression

Recombinant LreCAγ protein was obtained through a combination of bioinformatics and molecular biology techniques. Initially, the *LreCAγ* gene was identified using the Protein BLAST program, employing various bacterial γ-CA sequences as queries. The gene encoding LreCAγ was designed and synthesized by a specialized company, GeneArt (Life Technologies), before being cloned into the pET100/D-TOPO expression vector (Life Technologies). The recombinant LreCAγ protein was subsequently expressed in *E. coli* ArcticExpress competent cells and purified using a nickel-based His-Trap FF affinity column. Protein concentration was determined via Bradford assay, while purity was assessed by 12 % SDS-PAGE followed by Coomassie Brilliant Blue-R staining. The final protein yield was 90 %. Enzymatic activity was evaluated using a CA activity assay, which monitored pH changes during the conversion of CO_2 to HCO_3^- at 0 °C, quantified in Wilbur-Anderson units.

4.2. LreCAγ activity and inhibition/activation measurements

All tested anions, sulfonamides, sulfamides, sulfamates, amines, and amino acids were of the highest purity available from Merck (Milan, Italy). An Applied Photophysics stopped-flow instrument was used to assay the CA-catalyzed CO_2 hydration activity [60]. Phenol red (at a concentration of 0.2 mM) served as an indicator, operating at the absorbance maximum of 557 nm, with 20 mM TRIS (pH 8.3) buffer, and 20 mM $NaClO_4$ to maintain a constant ionic strength [74]. The initial rates of the CA-catalyzed CO_2 hydration reaction were followed for a period of 10–100 s. CO_2 concentrations ranged from 1.7 to 17 mM for determining the kinetic parameters and inhibition constants using Lineweaver–Burk plots [75–77]. At least six traces of the initial 5 %–10 % of the reaction were carried out to determine the initial velocity. Uncatalyzed rates were assessed similarly and subtracted from the total observed rates. Stock solutions of the inhibitor and activators (10–100 mM) were prepared in distilled-deionized water, and dilutions were subsequently made with the assay buffer. Inhibitor/activator and enzyme solutions were preincubated together for 15 min at room temperature to allow for the formation of the E-I (Enzyme-Inhibitor) or E-A (Enzyme-Activator) complex. Inhibition constants (K_I) were obtained by non-linear least-squares methods using GraphPad Prism 9 (San Diego, CA, USA) and the Cheng-Prusoff equation.

All reported inhibition constants and kinetic parameters for the uninhibited enzyme are the mean of at least three different determinations. The activation constant (K_A) values were obtained by considering the classical Michaelis-Menten equation, which has been fitted by non-linear least squares by using GraphPad Prism 9 (San Diego, CA, USA). All tested anions, sulfonamides, sulfamides, sulfamates, amines, and amino acids were of the highest purity available from Merck Italia (Milan, Italy).

4.3. Crystallographic studies

4.3.1. Crystallization and X-ray data collection

Initial crystallization trials were performed at 23 °C with a 10 mg/mL LreCAγ solution in Tris-HCl 50 mM, pH 9.0, using a commercially available crystallization screen (JCSG-plus™ from Molecular Dimensions). Crystals of LreCAγ were obtained using the sitting drop vapor diffusion method with 24-well Linbro plates. 2 μL of LreCAγ solution were mixed with 2 μL of a solution of 2.0 M ammonium sulfate, 0.1 M HEPES, pH 7.5, 2 % v/v PEG 400, and were equilibrated against the same solution at 296 K to obtain crystals in space group $P2_12_12_1$. 0.2 M magnesium formate dihydrate and 20 % w/v PEG3350 were equilibrated against the same solution at 296 K to obtain crystals in space group *I*222. All crystals were flash-frozen at 100 K using a solution obtained by adding 20 % (*v/v*) glycerol to the mother liquor solution as a cryoprotectant. Data on crystals of the complexes were collected using synchrotron radiation at the XRD2 beamline at Elettra Synchrotron (Trieste, Italy) with a wavelength of 1.00 Å and a DECTRIS Pilatus 6 M detector. Data were integrated and scaled using the program XDS [78]. Data processing statistics are shown in the Supporting Information.

4.3.2. Structure determination

The structure was solved by the molecular-replacement technique using the MOLREP program [79]and the coordinates generated from AlphaFold as a starting model. The model was refined using the REFMAC5 program [80] from the CCP4 suite [81]. Refinements proceeded using normal protocols of positional, isotropic, or anisotropic atomic displacement parameters alternating with the manual building of the models using COOT [82]. The quality of the final models was assessed with COOT and RAMPAGE [83]. Crystal parameters and refinement data are summarized in the Supporting Information. Atomic coordinates were deposited in the Protein Data Bank (PDB: 9SUZ and 9SUT). Graphical representations were generated with UCSF Chimera [84].

4.4. Effect on bacterial growth

4.4.1. Bacterial strains and culture conditions

E. coli DH5α was obtained from Agilent Technologies (Santa Clara, CA, USA) and cultured in Mueller-Hinton (MH) broth (Sigma-Aldrich, St. Louis, MO, USA) under aerobic conditions at 37 °C, with continuous shaking at 200 rpm in an INNOVA 42 incubator (Eppendorf, Hamburg, Germany). Overnight cultures were collected by centrifugation at 4 °C (1500×*g*, 30 min), resuspended in fresh MH broth to an initial optical density (OD) of 0.15 at 600 nm, and incubated until OD_{600} reached 0.6. Throughout the experiment, the pH of the medium was monitored to ensure optimal bacterial growth. Antibiotics were not introduced into the culture medium.

4.4.2. Bacterial growth monitoring and treatment with activators

Bacterial growth assays were performed in 96-well tissue culture-treated, clear polystyrene microplates (Falcon, Männedorf, Switzerland), with a total volume of 200 μL per well. The cultures were incubated at 37 °C with continuous agitation (80 rpm) on an integrated spectrophotometer plate reader (TECAN, Männedorf, Switzerland). Activators were administered at final concentrations of 0.1 and 1.0 μM during the exponential growth phase (OD_{600} = 0.5–0.6). Control conditions included untreated *E. coli* cultures as well as cultures treated with **AAZ** at a final concentration of 1 mg/mL. Each experiment was

performed in triplicate using independent biological replicates, and bacterial growth was monitored by measuring the OD_{600} at regular intervals using a SPARK multimode microplate reader (TECAN, Männedorf, Switzerland) [69].

4.5. Anti-inflammatory activity and biocompatibility evaluation

4.5.1. Human cell cultures

Undifferentiated human monocytes (CRL-3622™) were purchased from ATCC® and cultured in complete RPMI 1640 (Merck, Darmstadt, Germany) at 37 °C and 5 % CO_2. The medium was supplemented with 10 % of heat-inactivated foetal bovine serum (FBS, Gibco, Thermo Fisher Scientific, Waltham, MA, USA), 1 % penicillin/streptomycin (S.I. A.L. S.r.l., Rome, Italy), and 1 % sodium pyruvate (Merck, Darmstadt, Germany).

Human intestinal epithelial cells HIEC-6 (CRL-3266™) were purchased from ATCC® and cultured in complete DMEM/F12 (Merck, Darmstadt, Germany) at 37 °C and 5 % CO_2. The medium was supplemented with 20 mM HEPES (2-[4-(2-hydroxyethyl)piperazin-1-yl] ethanesulfonic acid, purchased from Merck, Darmstadt, Germany), 10 mM L-glutamine (Euroclone S.p.A., Milan, Italy), 10 ng/mL epidermal growth factor (EGF), 10 % heat-inactivated foetal bovine serum (FBS, Gibco, Thermo Fisher Scientific, Waltham, MA, USA), and 1 % penicillin/streptomycin (S.I.A.L. S.r.l., Rome, Italy) [85].

For differentiation into macrophages, monocytes were seeded in 96-well tissue culture-treated plates (Falcon®, Corning Incorporated, Brooklyn, NY, USA) and stimulated with 100 ng/mL of PMA (phorbol-12-myristate-13-acetate, purchased from Merck, Darmstadt, Germany, stock solution 1 mM in DMSO) in complete RPMI for 48 h at 37 °C and 5 % CO_2, as previously reported [86].

4.5.2. Cell metabolic activity

Undifferentiated monocytes were seeded in 96-well tissue culture-treated plates (Falcon®, Corning Incorporated, Brooklyn, NY, USA) at a density of 5×10^3 cells/well. Cultured cells were differentiated as previously described. After 48 h, the differentiation medium was discarded and replaced with a fresh one containing complete RPMI (UC, untreated cells) or selected compounds (**25**, **26**, **31**, **32**, **38**, **48**) at 0.1, 1, 10, 50, 100 μM (stock solutions: 100 mM in 1 % acetic acid for compounds **25**, **26** and **48**; 100 mM in 0.05 % HCl for compounds **31** and **32**; 100 mM in DMSO for compound **38**). To induce inflammation, macrophages were stimulated with LPS 0.5 μg/mL (lipopolysaccharide from *E. coli*, purchased from Merck, Darmstadt, Germany, stock solution 1 mg/mL in water) and exposed to compounds in parallel. After 24 h, the exposure media were replaced by 100 μL/well of fresh RPMI containing 3-(4,5-dimethylthiazol-2-yl)-2,5-diphenyltetrazolium bromide (MTT) 0.5 mg/mL (Merck, Darmstadt, Germany). Afterwards, cells were incubated for 4 h at 37 °C. Then, the MTT medium was discarded, and 100 μL of DMSO was added to each well. In the end, samples were incubated for 10 min at 37 °C.

HIEC-6 cells were seeded in 96-well tissue culture-treated plates (Falcon®, Corning Incorporated, Brooklyn, NY, USA) at a density of 5×10^3 cells/well. After 24 h, the medium was discarded, and cells were treated as described for macrophages. After 24 h and 48 h, the exposure media were replaced by 100 μL/well of fresh DMEM/F12 containing MTT 0.5 mg/mL (Merck, Darmstadt, Germany), and the MTT assay was performed as described previously in this section. The optical density in each well was measured at a wavelength of 540 nm using a spectrophotometer (Thermo Fisher Scientific, Waltham, MA, USA). Untreated cells (UC) were set as the control (100 % of cell metabolic activity). Each experiment was performed twice in triplicate per experimental condition ($n = 6$) [86].

4.5.3. Statistical analyses

Data were statistically analyzed by GraphPad Prism 8 (San Diego, CA, USA) using two-way analysis of variance (ANOVA) followed by Dunnett and Tukey's multiple comparison tests. The results are the mean values ± standard deviation (S.D.). Values of $p \leq 0.05$ were considered statistically significant.

CRediT authorship contribution statement

Alessandro Bonardi: Formal analysis. **Simone Carradori:** Writing – review & editing, Writing – original draft, Supervision, Funding acquisition, Formal analysis, Conceptualization. **Niccolò Paoletti:** Formal analysis. **Andrea Angeli:** Formal analysis. **Marta Ferraroni:** Formal analysis. **Damiano Iacovozzi:** Formal analysis. **Marialucia Gallorini:** Writing – original draft, Formal analysis. **Ilaria D'Agostino:** Writing – original draft, Formal analysis. **Viviana De Luca:** Formal analysis. **Paola Gratteri:** Writing – original draft, Supervision. **Amelia Cataldi:** Supervision, Funding acquisition, Conceptualization. **Claudiu T. Supuran:** Writing – review & editing, Conceptualization. **Clemente Capasso:** Writing – review & editing, Funding acquisition, Formal analysis, Conceptualization.

Abbreviations

AAZ, acetazolamide; ANOVA, analysis of variance; ATCC®, American Type Culture Collection; BLAST, Basic Local Alignment Search Tool; CA, carbonic anhydrase; CTX, cholera toxin; DMSO, dimethyl sulfoxide; DMEM/F12, Dulbecco's Modified Eagle Medium/Nutrient Mixture F-12; EGF, epidermal growth factor; FBS, fetal bovine serum; FF, fast flow (chromatography column type); HEPES, 2-[4-(2-hydroxyethyl)piperazin-1-yl]ethanesulfonic acid; HIEC-6, human intestinal epithelial cell line; IC_{50}, half-maximal inhibitory concentration; IPTG, isopropyl β-D-1-thiogalactopyranoside; K_A, activation constant; K_I, inhibition constant; kcat, catalytic turnover number; K_M, Michaelis–Menten constant; IBS, irritable bowel syndrome; LPS, lipopolysaccharide; MH, Mueller-Hinton; MTT, 3-(4,5-dimethylthiazol-2-yl)-2,5-diphenyltetrazolium bromide; OD_{600}, optical density at 600 nm; PMA, phorbol-12-myristate-13-acetate; SARs, structure–activity relationships; S.D., standard deviation; SDS-PAGE, sodium dodecyl sulfate–polyacrylamide gel electrophoresis; TRIS, tris(hydroxymethyl) aminomethane; UC, untreated cells.

Funding

S.C., C.C., and A.C. acknowledge financial support under the National Recovery and Resilience Plan (NRRP), Mission 4, Component 2, Investment 1.1, Call for tender n. 1409 published on 14/09/2022 by the Italian Ministry of University and Research (MUR), funded by the European Union – NextGenerationEU – Concession Decree No. 1409 of 14-09-2022 adopted by the Italian Ministry of University and Research, Project title "Activation of Carbonic Anhydrases encoded by the human probiotics to enhance gut microbiota performance against dysbiosis and microbial infections" - CUP: D53D23017140001 – Project code: P2022LX2RM.

S.C. and M.G. acknowledge financial support under the National Recovery and Resilience Plan (NRRP), Mission 4, Component 2, Investment 1.5, Call for tender n. 51/2024 published on 19/01/2024 by the BANDO A CASCATA PER UNIVERSITÀ, ENTI PUBBLICI DI RICERCA E ALTRI ORGANISMI DI RICERCA Progetto "THE - Tuscany Health Ecosystem", funded by the European Union – NextGenerationEU – Concession Decree No. 3277 of 30-12-2021 adopted by the Italian Ministry of University and Research, Project title "Impatto della Modulazione delle Anidrasi Carboniche del Microbiota Intestinale sull'Asse

Intestino-Cervello" MACMI - CUP: D73C24000960003 – Project code: ECS00000017.

Declaration of competing interest

The authors declare that they have no known competing financial interests or personal relationships that could have appeared to influence the work reported in this paper.

Acknowledgment

This article is based upon work from COST Action EURESTOP, CA21145, supported by COST (European Cooperation in Science and Technology) to S.C., M.G., and I.D.A. We also gratefully acknowledge Elettra and XRD2 beamline for providing beamtime and support under proposal 20220596, and we would like to thank Dr. Nicola Demitri for assistance and support in using the beamline.

Appendix A. Supplementary data

Supplementary data to this article can be found online at https://doi.org/10.1016/j.ejmech.2025.118291.

Data availability

Data will be made available on request.

References

[1] H.T. John, T.C. Thomas, E.C. Chukwuebuka, A.B. Ali, R. Anass, Y.Y. Tefera, B. Babu, N. Negrut, A. Ferician, P. Marian, The microbiota–human health axis, Microorganisms 13 (2025) 948, https://doi.org/10.3390/microorganisms13040948.

[2] S. Han, E.R. Guiberson, Y. Li, J.L. Sonnenburg, High-throughput identification of gut microbiome-dependent metabolites, Nat. Protoc. 19 (2024) 2180–2205, https://doi.org/10.1038/s41596-024-00980-6.

[3] W.K. Mousa, S. Mousa, R. Ghemrawi, D. Obaid, M. Sarfraz, F. Chehadeh, S. Husband, Probiotics modulate host immune response and interact with the gut microbiota: shaping their composition and mediating antibiotic resistance, Int. J. Mol. Sci. 24 (2023) 13783, https://doi.org/10.3390/ijms241813783.

[4] A. Latif, A. Shehzad, S. Niazi, A. Zahid, W. Ashraf, M.W. Iqbal, A. Rehman, T. Riaz, R.M. Aadil, I.M. Khan, F. Özogul, J.M. Rocha, T. Esatbeyoglu, S.A. Korma, Probiotics: mechanism of action, health benefits and their application in food industries, Front. Microbiol. 14 (2023) 1216674, https://doi.org/10.3389/fmicb.2023.1216674.

[5] T. Wilkins, J. Sequoia, Probiotics for gastrointestinal conditions: a summary of the evidence, Am. Fam. Physician 96 (2017) 170–178.

[6] M. You, N. Chen, Y. Yang, L. Cheng, H. He, Y. Cai, Y. Liu, H. Liu, G. Hong, The gut microbiota–brain axis in neurological disorders, MedComm 5 (2024) (2020) e656, https://doi.org/10.1002/mco2.656.

[7] S. Ashique, S. Mohanto, M.G. Ahmed, N. Mishra, A. Garg, D.K. Chellappan, T. Omara, S. Iqbal, I. Kahwa, Gut-brain axis: a cutting-edge approach to target neurological disorders and potential synbiotic application, Heliyon 10 (2024) e34092, https://doi.org/10.1016/j.heliyon.2024.e34092.

[8] C. Purdel, A. Ungurianu, I. Adam-Dima, D. Margină, Exploring the potential impact of probiotic use on drug metabolism and efficacy, Biomed. Pharmacother. 161 (2023) 114468, https://doi.org/10.1016/j.biopha.2023.114468.

[9] S. Sarkar, Potential of probiotics as pharmaceutical agent: a review, Br. Food J. 115 (2013) 1658–1687, https://doi.org/10.1108/BFJ-06-2011-0163.

[10] MdR. Amin, A.P. Biswas, M. Tasnim, MdN. Islam, MdS. Azam, Probiotics and their applications in functional foods: a health perspective, Appl. Food Res. 5 (2025) 101193, https://doi.org/10.1016/j.afres.2025.101193.

[11] M. Cunningham, M.A. Azcarate-Peril, A. Barnard, V. Benoit, R. Grimaldi, D. Guyonnet, H.D. Holscher, K. Hunter, S. Manurung, D. Obis, M.I. Petrova, R. E. Steinert, K.S. Swanson, D. van Sinderen, J. Vulevic, G.R. Gibson, Shaping the future of probiotics and prebiotics, Trends Microbiol. 29 (2021) 667–685, https://doi.org/10.1016/j.tim.2021.01.003.

[12] M. Abdul Manan, Progress in probiotic science: prospects of functional probiotic-based foods and beverages, Int. J. Food Sci. 2025 (2025) 5567567, https://doi.org/10.1155/ijfo/5567567.

[13] L. Zhao, M. Niu, Z. Ma, F. He, X. Liu, X. Gong, Z. Chai, Z. Wang, Q. Feng, L. Wang, Modified probiotics and the related combinatorial therapeutics, Acta Pharm. Sin. B 15 (2025) 2431–2453, https://doi.org/10.1016/j.apsb.2025.03.021.

[14] A. Minocha, Probiotics for preventive health, Nutr. Clin. Pract. 24 (2009) 227–241, https://doi.org/10.1177/0884533608331177.

[15] D.J. Merenstein, D.J. Tancredi, J.P. Karl, A.H. Krist, I. Lenoir-Wijnkoop, G. Reid, S. Roos, H. Szajewska, M.E. Sanders, Is there evidence to support probiotic use for healthy people? Adv. Nutr. 15 (2024) 100265 https://doi.org/10.1016/j.advnut.2024.100265.

[16] C.T. Supuran, Carbonic anhydrases–an overview, Curr. Pharm. Des. 14 (2008) 603–614, https://doi.org/10.2174/138161208783877884.

[17] C. Capasso, C.T. Supuran, Targeting carbonic anhydrases, in: Targeting Carbonic Anhydrases, Future Science Ltd, 2014, pp. 2–4, https://doi.org/10.4155/fseb2013.13.45.

[18] P. Singh, M. Arifuddin, C.T. Supuran, S.G. Nerella, Carbonic anhydrase inhibitors: structural insights and therapeutic potential, Bioorg. Chem. 156 (2025) 108224, https://doi.org/10.1016/j.bioorg.2025.108224.

[19] A. Bonardi, C.T. Supuran, Polypharmacology of carbonic anhydrase inhibitors and activators, Expet Opin. Pharmacother. 26 (2025) 567–580, https://doi.org/10.1080/14656566.2025.2474574.

[20] H. Aslan, G. Renzi, A. Angeli, I. D'Agostino, R. Ronca, M. Massardi, C. Tavani, S. Carradori, M. Ferraroni, P. Governa, F. Manetti, F. Carta, C. Supuran, Benzenesulfonamide decorated dihydropyrimidin(thi)ones: carbonic anhydrase profiling and antiproliferative activity, RSC Med. Chem. 15 (2024) 1929–1941, https://doi.org/10.1039/D4MD00101J.

[21] D.A. Anakök, A. Angeli, I. D'Agostino, G. Renzi, M.L. Massardi, C. Tavani, S. Çete, S. Carradori, R. Ronca, C. Capasso, F. Carta, C.T. Supuran, A journey around boronic acids: sulfonyl hydrazone-containing derivatives as carbonic anhydrase inhibitors, Chem. Biol. Drug Des. 105 (2025) e70108, https://doi.org/10.1111/cbdd.70108.

[22] I. D'Agostino, S. Zara, S. Carradori, V. DeLuca, C. Clemente, C.H.M. Kocken, A.-M. Zeeman, A. Angeli, F. Carta, C.T. Supuran, Antimalarial agents targeting Plasmodium falciparum carbonic anhydrase: towards dual acting artesunate hybrid compounds, ChemMedChem 18 (2023) e202300267, https://doi.org/10.1002/cmdc.202300267.

[23] G. Benito, I. D'Agostino, S. Carradori, M. Fantacuzzi, M. Agamennone, V. Puca, R. Grande, C. Capasso, F. Carta, C.T. Supuran, Erlotinib-containing benzenesulfonamides as anti-helicobacter pylori agents through carbonic anhydrase inhibition, Future Med. Chem. 15 (2023) 1865–1883, https://doi.org/10.4155/fmc-2023-0208.

[24] M. Fantacuzzi, I. D'Agostino, S. Carradori, F. Liguori, F. Carta, M. Agamennone, A. Angeli, F. Sannio, J.-D. Docquier, C. Capasso, C.T. Supuran, Benzenesulfonamide derivatives as Vibrio cholerae carbonic anhydrases inhibitors: a computational-aided insight in the structural rigidity-activity relationships, J. Enzym. Inhib. Med. Chem. 38 (2023) 2201402, https://doi.org/10.1080/14756366.2023.2201402.

[25] W.M. Eldehna, A.A. El-Hamaky, S. Giovannuzzi, Z.M. Elsayed, M.A. Alkabbani, E. F. Khaleel, M.M. Al-Sanea, M.F. Abo-Ashour, Y.S.R. Elnaggar, A. Nocentini, C. T. Supuran, H.O. Tawfik, Development of isatin-functionalized benzenesulfonamides as novel carbonic anhydrase II and VII inhibitors with antiepileptic potential, Eur. J. Med. Chem. 292 (2025) 117706, https://doi.org/10.1016/j.ejmech.2025.117706.

[26] S. Giovannuzzi, D. Chavarria, G. Provensi, M. Leri, M. Bucciantini, S. Carradori, A. Bonardi, P. Gratteri, F. Borges, A. Nocentini, C.T. Supuran, Dual inhibitors of brain carbonic anhydrases and monoamine Oxidase-B efficiently protect against Amyloid-β-Induced neuronal toxicity, oxidative stress, and mitochondrial dysfunction, J. Med. Chem. 67 (2024) 4170–4193, https://doi.org/10.1021/acs.jmedchem.4c00045.

[27] G. Provensi, A. Costa, B. Rani, M.V. Becagli, F. Vaiano, M.B. Passani, D. Tanini, A. Capperucci, S. Carradori, J.P. Petzer, A. Petzer, D. Vullo, G. Costantino, P. Blandina, A. Angeli, C.T. Supuran, New β-arylchalcogeno amines with procognitive properties targeting carbonic anhydrases and monoamine oxidases, Eur. J. Med. Chem. 244 (2022) 114828, https://doi.org/10.1016/j.ejmech.2022.114828.

[28] M. Tugrak, H.I. Gul, K. Bandow, H. Sakagami, I. Gulcin, Y. Ozkay, C.T. Supuran, Synthesis and biological evaluation of some new mono Mannich bases with piperazines as possible anticancer agents and carbonic anhydrase inhibitors, Bioorg. Chem. 90 (2019) 103095, https://doi.org/10.1016/j.bioorg.2019.103095.

[29] İ. Gülçin, B. Trofimov, R. Kaya, P. Taslimi, L. Sobenina, E. Schmidt, O. Petrova, S. Malysheva, N. Gusarova, V. Farzaliyev, A. Sujayev, S. Alwasel, C.T. Supuran, Synthesis of nitrogen, phosphorus, selenium and sulfur-containing heterocyclic compounds - determination of their carbonic anhydrase, acetylcholinesterase, butyrylcholinesterase and α-glycosidase inhibition properties, Bioorg. Chem. 103 (2020) 104171, https://doi.org/10.1016/j.bioorg.2020.104171.

[30] C.T. Supuran, Multi- and polypharmacology of carbonic anhydrase inhibitors, Pharmacol. Rev. 77 (2025) 100004, https://doi.org/10.1124/pharmrev.124.001125.

[31] C. Capasso, C.T. Supuran, Overview on bacterial carbonic anhydrase genetic families, Enzymes 55 (2024) 1–29, https://doi.org/10.1016/bs.enz.2024.05.004.

[32] C.T. Supuran, C. Capasso, An overview of the bacterial carbonic anhydrases, Metabolites 7 (2017) 56, https://doi.org/10.3390/metabo7040056.

[33] B.L. Bernardoni, C. La Motta, S. Carradori, I. D'Agostino, Helicobacter pylori CAs inhibition, Enzymes 55 (2024) 213–241, https://doi.org/10.1016/bs.enz.2024.05.013.

[34] A. Gumus, I. D'Agostino, V. Puca, V. Crocetta, S. Carradori, L. Cutarella, M. Mori, F. Carta, A. Angeli, C. Capasso, C.T. Supuran, Cyclization of acyl thiosemicarbazides led to new Helicobacter pylori α-carbonic anhydrase inhibitors, Arch. Pharm. 357 (2024) e2400548, https://doi.org/10.1002/ardp.202400548.

[35] I. D'Agostino, G.E. Mathew, P. Angelini, R. Venanzoni, G. Angeles Flores, A. Angeli, S. Carradori, B. Marinacci, L. Menghini, M.A. Abdelgawad, M. M. Ghoneim, B. Mathew, C.T. Supuran, Biological investigation of N-methyl thiosemicarbazones as antimicrobial agents and bacterial carbonic anhydrases inhibitors, J. Enzym. Inhib. Med. Chem. 37 (2022) 986–993, https://doi.org/10.1080/14756366.2022.2055009.

[36] F. Melfi, I. D'Agostino, S. Carradori, F. Carta, A. Angeli, G. Costa, G. Renzi, A. Čikoš, D. Vullo, J. Rešetar, M. Ferraroni, C. Baroni, F. Mancuso, R. Gitto, F. A. Ambrosio, E. Marchese, R. Torcasio, N. Amodio, C. Capasso, S. Alcaro, C. T. Supuran, O-derivatization of natural tropolone and β-thujaplicin leading to effective inhibitors of human carbonic anhydrases IX and XII, Eur. J. Med. Chem. 290 (2025) 117552, https://doi.org/10.1016/j.ejmech.2025.117552.
[37] C. Capasso, C.T. Supuran, Biomedical applications of prokaryotic carbonic anhydrases: an update, Expert Opin. Ther. Pat. 34 (2024) 351–363, https://doi.org/10.1080/13543776.2024.2365407.
[38] C. Capasso, C.T. and Supuran, Carbonic anhydrase and bacterial metabolism: a chance for antibacterial drug discovery, Expert Opin. Ther. Pat. 34 (2024) 465–474, https://doi.org/10.1080/13543776.2024.2332663.
[39] R. Grande, S. Carradori, V. Puca, I. Vitale, A. Angeli, A. Nocentini, A. Bonardi, P. Gratteri, P. Lanuti, G. Bologna, P. Simeone, C. Capasso, V. De Luca, C. T. Supuran, Selective inhibition of Helicobacter pylori carbonic anhydrases by carvacrol and thymol could impair biofilm production and the release of outer membrane vesicles, Int. J. Mol. Sci. 22 (2021) 11583, https://doi.org/10.3390/ijms222111583.
[40] M.S. Gheibzadeh, C. Capasso, C.T. Supuran, R. Zolfaghari Emameh, Antibacterial carbonic anhydrase inhibitors targeting Vibrio cholerae enzymes, Expert Opin. Ther. Targets 28 (2024) 623–635, https://doi.org/10.1080/14728222.2024.2369622.
[41] S. Del Prete, S. Isik, D. Vullo, V. De Luca, V. Carginale, A. Scozzafava, C.T. Supuran, C. Capasso, DNA cloning, characterization, and inhibition studies of an α-Carbonic anhydrase from the pathogenic bacterium Vibrio cholerae, J. Med. Chem. 55 (2012) 10742–10748, https://doi.org/10.1021/jm301611m.
[42] A. Bonardi, A. Nocentini, S.M. Osman, F.A. Alasmary, T.M. Almutairi, D. S. Abdullah, P. Gratteri, C.T. Supuran, Inhibition of α-, β- and γ-carbonic anhydrases from the pathogenic bacterium Vibrio cholerae with aromatic sulphonamides and clinically licenced drugs – a joint docking/molecular dynamics study, J. Enzym. Inhib. Med. Chem. 36 (2021) 469–479, https://doi.org/10.1080/14756366.2020.1862102.
[43] F. Mancuso, L. De Luca, A. Angeli, E. Berrino, S. Del Prete, C. Capasso, C. T. Supuran, R. Gitto, In silico-guided identification of new potent inhibitors of carbonic anhydrases expressed in Vibrio cholerae, ACS Med. Chem. Lett. 11 (2020) 2294–2299, https://doi.org/10.1021/acsmedchemlett.0c00417.
[44] A. Amedei, C. Capasso, G. Nannini, C.T. Supuran, Microbiota, bacterial carbonic anhydrases, and modulators of their activity: links to human diseases? Mediat. Inflamm. 2021 (2021) 6926082 https://doi.org/10.1155/2021/6926082.
[45] L.J. Urbański, S. Bua, A. Angeli, R.Z. Emameh, H.R. Barker, M. Kuuslahti, V. P. Hytönen, S. Parkkila, C.T. Supuran, The production and biochemical characterization of α-carbonic anhydrase from Lactobacillus rhamnosus GG, Appl. Microbiol. Biotechnol. 106 (2022) 4065–4074, https://doi.org/10.1007/s00253-022-11990-3.
[46] D. Vullo, S. Del Prete, S.M. Osman, F.A.S. Alasmary, Z. AlOthman, W.A. Donald, C. Capasso, C.T. Supuran, Comparison of the amine/amino acid activation profiles of the β- and γ-carbonic anhydrases from the pathogenic bacterium Burkholderia pseudomallei, J. Enzym. Inhib. Med. Chem. 33 (2018) 25–30, https://doi.org/10.1080/14756366.2017.1387544.
[47] C.T. Supuran, Carbonic anhydrase inhibition/activation: trip of a scientist around the world in the search of novel chemotypes and drug targets, Curr. Pharm. Des. 16 (2010) 3233–3245, https://doi.org/10.2174/138161210793429797.
[48] A. Angeli, E. Berrino, S. Carradori, C.T. Supuran, M. Cirri, F. Carta, G. Costantino, Amine- and amino acid-based compounds as carbonic anhydrase activators, Molecules 26 (2021) 7331, https://doi.org/10.3390/molecules26237331.
[49] A. Angeli, S. Del Prete, S.M. Osman, F.A.S. Alasmary, Z. AlOthman, W.A. Donald, C. Capasso, C.T. Supuran, Activation studies of the α- and β-carbonic anhydrases from the pathogenic bacterium Vibrio cholerae with amines and amino acids, J. Enzym. Inhib. Med. Chem. 33 (2017) 227–233, https://doi.org/10.1080/14756366.2017.1412316.
[50] A. Angeli, S. Del Prete, M. Pinteala, S.S. Maier, W.A. Donald, B.C. Simionescu, C. Capasso, C.T. Supuran, The first activation study of the β-carbonic anhydrases from the pathogenic bacteria Brucella suis and Francisella tularensis with amines and amino acids, J. Enzym. Inhib. Med. Chem. 34 (2019) 1178–1185, https://doi.org/10.1080/14756366.2019.1630617.
[51] A. Stefanucci, A. Angeli, M.P. Dimmito, G. Luisi, S. Del Prete, C. Capasso, W. A. Donald, A. Mollica, C.T. Supuran, Activation of β- and γ-carbonic anhydrases from pathogenic bacteria with tripeptides, J. Enzym. Inhib. Med. Chem. 33 (2018) 945–950, https://doi.org/10.1080/14756366.2018.1468530.
[52] A. Angeli, S. Del Prete, S.M. Osman, Z. AlOthman, W.A. Donald, C. Capasso, C. T. Supuran, Activation studies of the γ-Carbonic anhydrases from the antarctic marine bacteria Pseudoalteromonas haloplanktis and Colwellia psychrerythraea with amino acids and amines, Mar. Drugs 17 (2019) 238, https://doi.org/10.3390/md17040238.
[53] A. Angeli, S. Del Prete, W.A. Donald, C. Capasso, C.T. Supuran, The γ-carbonic anhydrase from the pathogenic bacterium Vibrio cholerae is potently activated by amines and amino acids, Bioorg. Chem. 77 (2018) 1–5, https://doi.org/10.1016/j.bioorg.2018.01.003.
[54] J. Abuqwider, M. Altamimi, G. Mauriello, Limosilactobacillus reuteri in health and disease, Microorganisms 10 (2022) 522, https://doi.org/10.3390/microorganisms10030522.
[55] A.H. Lee, D.M. Rodriguez Jimenez, M. Meisel, Limosilactobacillus reuteri - a probiotic gut commensal with contextual impact on immunity, Gut Microbes 17 (2025) 2451088, https://doi.org/10.1080/19490976.2025.2451088.
[56] C.T. Supuran, Carbonic anhydrases: novel therapeutic applications for inhibitors and activators, Nat. Rev. Drug Discov. 7 (2008) 168–181, https://doi.org/10.1038/nrd2467.
[57] S. Del Prete, D. Vullo, V. De Luca, V. Carginale, S.M. Osman, Z. AlOthman, C. T. Supuran, C. Capasso, Comparison of the sulfonamide inhibition profiles of the α-, β- and γ-carbonic anhydrases from the pathogenic bacterium Vibrio cholerae, Bioorg. Med. Chem. Lett 26 (2016) 1941–1946, https://doi.org/10.1016/j.bmcl.2016.03.014.
[58] S. Del Prete, S. Bua, C.T. Supuran, C. Capasso, Escherichia coli γ-carbonic anhydrase: characterisation and effects of simple aromatic/heterocyclic sulphonamide inhibitors, J. Enzym. Inhib. Med. Chem. 35 (2020) 1545–1554, https://doi.org/10.1080/14756366.2020.1800670.
[59] M. Ferraroni, A. Angeli, V. De Luca, C. Capasso, C.T. Supuran, Kinetic and structural studies of gamma-carbonic anhydrase from the oral pathogen Porphyromonas gingivalis, J. Struct. Biol. 217 (2025) 108154, https://doi.org/10.1016/j.jsb.2024.108154.
[60] R.G. Khalifah, The carbon dioxide hydration activity of carbonic anhydrase. I. Stop-flow kinetic studies on the native human isoenzymes B and C, J. Biol. Chem. 246 (1971) 2561–2573.
[61] A. Nocentini, A. Angeli, F. Carta, J.-Y. Winum, R. Zalubovskis, S. Carradori, C. Capasso, W.A. Donald, C.T. Supuran, Reconsidering anion inhibitors in the general context of drug design studies of modulators of activity of the classical enzyme carbonic anhydrase, J. Enzym. Inhib. Med. Chem. 36 (2021) 561–580, https://doi.org/10.1080/14756366.2021.1882453.
[62] K. D'Ambrosio, A. Di Fiore, V. Alterio, E. Langella, S.M. Monti, C.T. Supuran, G. De Simone, Multiple binding modes of inhibitors to human carbonic anhydrases: an update on the design of isoform-specific modulators of activity, Chem. Rev. (2024), https://doi.org/10.1021/acs.chemrev.4c00278.
[63] J. Herrou, S. Crosson, Molecular structure of the Brucella abortus metalloprotein RicA, a Rab2-binding virulence effector, Biochemistry 52 (2013) 9020–9028, https://doi.org/10.1021/bi401373r.
[64] J. Jeyakanthan, S. Rangarajan, P. Mridula, S.P. Kanaujia, Y. Shiro, S. Kuramitsu, S. Yokoyama, K. Sekar, Observation of a calcium-binding site in the gamma-class carbonic anhydrase from Pyrococcus horikoshii, Acta Crystallogr. D Biol. Crystallogr. 64 (2008) 1012–1019, https://doi.org/10.1107/S0907444908024323.
[65] H.-M. Park, J.-H. Park, J.-W. Choi, J. Lee, B.Y. Kim, C.-H. Jung, J.-S. Kim, Structures of the γ-class carbonic anhydrase homologue YrdA suggest a possible allosteric switch, Acta Crystallogr. D Biol. Crystallogr. 68 (2012) 920–926, https://doi.org/10.1107/S0907444912017210.
[66] M. Vogler, R. Karan, D. Renn, A. Vancea, M.-T. Vielberg, S.W. Grötzinger, P. DasSarma, S. DasSarma, J. Eppinger, M. Groll, M. Rueping, Crystal structure and active site engineering of a halophilic γ-Carbonic anhydrase, Front. Microbiol. 11 (2020) 742, https://doi.org/10.3389/fmicb.2020.00742.
[67] T.M. Iverson, B.E. Alber, C. Kisker, J.G. Ferry, D.C. Rees, A closer look at the active site of gamma-class carbonic anhydrases: high-resolution crystallographic studies of the carbonic anhydrase from Methanosarcina thermophila, Biochemistry 39 (2000) 9222–9231, https://doi.org/10.1021/bi000204s.
[68] A. Di Fiore, V. De Luca, E. Langella, A. Nocentini, M. Buonanno, S.M. Monti, C. T. Supuran, C. Capasso, G. De Simone, Biochemical, structural, and computational studies of a γ-carbonic anhydrase from the pathogenic bacterium Burkholderia pseudomallei, Comput. Struct. Biotechnol. J. 20 (2022) 4185–4194, https://doi.org/10.1016/j.csbj.2022.07.033.
[69] V. De Luca, V. Carginale, C.T. Supuran, C. Capasso, The gram-negative bacterium Escherichia coli as a model for testing the effect of carbonic anhydrase inhibition on bacterial growth, J. Enzym. Inhib. Med. Chem. 37 (2022) 2092–2098, https://doi.org/10.1080/14756366.2022.2101644.
[70] S. Del Prete, V. De Luca, A. Nocentini, A. Scaloni, M.D. Mastrolorenzo, C. T. Supuran, C. Capasso, Anion inhibition studies of the beta-carbonic anhydrase from Escherichia coli, Molecules 25 (2020) 2564, https://doi.org/10.3390/molecules25112564.
[71] A. Nocentini, S. Del Prete, M.D. Mastrolorenzo, W.A. Donald, C. Capasso, C. T. Supuran, Activation studies of the β-carbonic anhydrases from Escherichia coli with amino acids and amines, J. Enzym. Inhib. Med. Chem. 35 (2020) 1379–1386, https://doi.org/10.1080/14756366.2020.1781845.
[72] J.D. Cronk, J.A. Endrizzi, M.R. Cronk, J.W. O'neill, K.Y. Zhang, Crystal structure of E. coli beta-carbonic anhydrase, an enzyme with an unusual pH-dependent activity, Protein Sci. 10 (2001) 911–922, https://doi.org/10.1110/ps.46301.
[73] C. Merlin, M. Masters, S. McAteer, A. Coulson, Why is carbonic anhydrase essential to Escherichia coli? J. Bacteriol. 185 (2003) 6415–6424, https://doi.org/10.1128/JB.185.21.6415-6424.2003.
[74] O. Akgul, A. Angeli, S. Selleri, C. Capasso, C.T. Supuran, F. Carta, Taurultams incorporating arylsulfonamide: first in vitro inhibition studies of α-, β- and γ-class carbonic anhydrases from Vibrio cholerae and Burkholderia pseudomallei, Eur. J. Med. Chem. 219 (2021) 113444, https://doi.org/10.1016/j.ejmech.2021.113444.
[75] I. Nishimori, T. Minakuchi, K. Morimoto, S. Sano, S. Onishi, H. Takeuchi, D. Vullo, A. Scozzafava, C.T. Supuran, Carbonic anhydrase inhibitors: DNA cloning and inhibition studies of the alpha-carbonic anhydrase from Helicobacter pylori, a new target for developing sulfonamide and sulfamate gastric drugs, J. Med. Chem. 49 (2006) 2117–2126, https://doi.org/10.1021/jm0512600.
[76] I. D'Agostino, A. Bonardi, M. Ferraroni, P. Gratteri, A. Angeli, C.T. Supuran, Exploring the polypharmacological potential of PCI-27483: a selective inhibitor of carbonic anhydrases IX and XII, ACS Med. Chem. Lett. 15 (2024) 2042–2045, https://doi.org/10.1021/acsmedchemlett.4c00443.
[77] C. Baroni, I. D'Agostino, G. Renzi, J.T. Kilbile, Y. Tamboli, M. Ferraroni, S. Carradori, C. Capasso, F. Carta, C.T. Supuran, Lasamide, a potent human

carbonic anhydrase inhibitor from the market: inhibition profiling and crystallographic studies, ACS Med. Chem. Lett. 15 (2024) 1749–1755, https://doi.org/10.1021/acsmedchemlett.4c00341.
[78] A.G.W. Leslie, H.R. Powell, Processing diffraction data with mosflm, in: R.J. Read, J.L. Sussman (Eds.), Evolving Methods for Macromolecular Crystallography, Springer Netherlands, Dordrecht, 2007, pp. 41–51, https://doi.org/10.1007/978-1-4020-6316-9_4.
[79] A. Vagin, A. Teplyakov, Molecular replacement with MOLREP, Acta Crystallogr. D 66 (2010) 22–25, https://doi.org/10.1107/S0907444909042589.
[80] G.N. Murshudov, P. Skubák, A.A. Lebedev, N.S. Pannu, R.A. Steiner, R.A. Nicholls, M.D. Winn, F. Long, A.A. Vagin, REFMAC5 for the refinement of macromolecular crystal structures, Acta Crystallogr. D Biol. Crystallogr. 67 (2011) 355–367, https://doi.org/10.1107/S0907444911001314.
[81] M.A. Hough, K.S. Wilson, From crystal to structure with CCP4, Acta Crystallogr. D Struct. Biol. 74 (2018) 67, https://doi.org/10.1107/S2059798317017557.
[82] P. Emsley, B. Lohkamp, W.G. Scott, K. Cowtan, Features and development of coot, Acta Crystallogr. D Biol. Crystallogr. 66 (2010) 486–501, https://doi.org/10.1107/S0907444910007493.
[83] S.C. Lovell, I.W. Davis, W.B. Arendall III, P.I.W. de Bakker, J.M. Word, M. G. Prisant, J.S. Richardson, D.C. Richardson, Structure validation by Cα geometry: ϕ,ψ and Cβ deviation, proteins: structure, Funct. Bioinf. 50 (2003) 437–450, https://doi.org/10.1002/prot.10286.
[84] E.F. Pettersen, T.D. Goddard, C.C. Huang, G.S. Couch, D.M. Greenblatt, E.C. Meng, T.E. Ferrin, UCSF Chimera–a visualization system for exploratory research and analysis, J. Comput. Chem. 25 (2004) 1605–1612, https://doi.org/10.1002/jcc.20084.
[85] F. Melfi, M. Fantacuzzi, S. Carradori, I. D'Agostino, A. Ammazzalorso, N. Mencarelli, M. Gallorini, M. Spano, P. Guglielmi, M. Agamennone, S. Haji Ali, A. Al-Samydai, F. Sisto, Azo derivatives of monoterpenes as anti-helicobacter pylori agents: from synthesis to structure-based target investigation, RSC Med. Chem. (2024), https://doi.org/10.1039/d4md00511b.
[86] M. Gallorini, S. Carradori, D.I.S.P. Resende, L. Saso, A. Ricci, A. Palmeira, A. Cataldi, M. Pinto, E. Sousa, Natural and synthetic xanthone derivatives counteract oxidative stress via Nrf2 modulation in inflamed human macrophages, Int. J. Mol. Sci. 23 (2022) 13319, https://doi.org/10.3390/ijms232113319.